

On the particularities of the forced vibration of the hydro-elastic system consisting of a moving elastic plate, compressible viscous fluid and rigid wall

Surkay D. Akbarov^{*1,2} and Panakh G. Panakhli^{3a}

¹*Yildiz Technical University, Faculty of Mechanical Engineering, Department of Mechanical Engineering, Yildiz Campus, 34349, Besiktas, Istanbul, Turkey*

²*Institute of Mathematics and Mechanics of the National Academy of Sciences of Azerbaijan, 37041, Baku, Azerbaijan*

³*Azerbaijan Architecture and Civil Engineering University, Faculty of Mechanical and Information Technologies, Department of Computer Hardware and Software, Baku, Azerbaijan*

(Received January 13, 2017, Revised May 6, 2017, Accepted June 19, 2017)

Abstract. This paper studies the particularities of the forced vibration of the hydro-elastic system consisting of a moving elastic plate, compressible viscous fluid and rigid wall. This study is made by employing the discrete-analytical solution method proposed in the paper by the authors (Akbarov and Panakhli (2015)). It is assumed that in the initial state the fluid flow is caused by the axial movement of the plate and the additional lineally-located time-harmonic forces act on the plate and these forces cause additional flow field in the fluid and a stress-strain state in the plate. The stress-strain state in the plate is described by utilizing the exact equations and relations of the linear elastodynamics. However, the additional fluid flow field is described with linearized Navier-Stokes equations for a compressible viscous fluid. Numerical results related to the influence of the problem parameters on the frequency response of the normal stress acting on the plate fluid interface plane and fluid flow velocity on this plane are presented and discussed. In this discussion, attention is focused on the influence of the initial plate axial moving velocity on these responses. At the same, it is established that as a result of the plate moving a resonance type of phenomenon can take place under forced vibration of the system. Moreover, numerical results regarding the influence of the fluid compressibility on these responses are also presented and discussed.

Keywords: compressible viscous fluid; elastic plate; frequency response; critical frequency; moving plate; forced vibration

1. Introduction

The investigations on the fluid-plate interaction are required by the modern levels of development of the aeronautical, astronautical, nuclear, chemical, biological, mechanical and civil engineering. The first attempt in this field was made approximately hundred years ago by Lamb

*Corresponding author, Professor, E-mail: akbarov@yildiz.edu.tr

^aPh.D., E-mail: panahli.panah@gmail.com

(1921) in which vibrations of a circular elastic “baffled” plate in contact with still water, which was modeled as inviscid fluid, were studied. It used the so-called “non-dimensional added virtual mass incremental” (NAVMI) method which has also been employed for the solution to plate-fluid interaction problems. This method supposed that the modes of vibration of the plate in contact with still water are the same as those in a vacuum, and the natural frequency is determined by the use of the Rayleigh quotient. According to this quotient, natural frequencies of the plate are equated to the ratio between the maximum potential energy of the plate and the sum of the kinetic energies of both the plate and the fluid. In future the NAVMI method has also been employed in many related investigations such as in papers by Kwak and Kim (1991), Fu and Price (1987), Zhao and Yu (2012) and in many others listed therein. It should also be noted that there have also been investigations (see, for instance, papers by Tubaldi and Armabili (2013), Charman and Sorokin (2005) and others listed therein) which have been carried out without employing the NAVMI method.

Another type plate-fluid interaction problems relate to the study of a wave propagation in corresponding hydro-elastic systems. These studies are made in a paper by Sorokin and Chubinskij (2008) and others listed therein. Note that before this paper the problems of time harmonic linear wave propagation in plate-fluid system were investigated within the framework of the theory of compressible inviscid fluid. Sorokin and Chubinskij (2008) also first investigated the role of fluid viscosity in wave propagation in the mentioned system. However, in this paper and all the papers indicated above, the equations of motion of the plate were written within the scope of approximate plate theories using various types of hypotheses, such as the Kirchhoff hypothesis for plates. At the same time, in the foregoing investigations (except the paper by Zhao and Yu (2012)) the initial strains (or stresses) in plates, which can be one of their reference characteristics, were not taken into account. These two characteristics, namely the use of the exact equations of plate motion and the existence of initial stresses in the plate were taken into consideration in a paper by Bagno (2015), Bagno *et al.* (1994) and others, a review of which is given in a survey paper by Bagno and Guz (1997). Note that in these papers, in studying wave propagation in pre-stressed plate+compressible viscous fluid systems, the motion of the plate was written within the scope of the so-called three-dimensional linearized theory of elastic waves in initially-stressed bodies. However, the motion of the viscous fluid was written within the scope of the linearized Navier-Stokes equations. Detailed consideration of related results was made in the monograph by Guz (2009).

Until recently, within this framework, there has been no investigation related to the forced vibration of the pre-strained plate+compressible viscous fluid system. The first attempts in these fields were made in the papers by Akbarov and Ismailov (2014, 2017). Note that the paper by Akbarov and Ismailov (2014) deals with the study of the forced vibration of the hydro-elastic system consisting of the pre-strained highly elastic plate and compressible viscous fluid filling a half-plane. However, the paper by Akbarov and Ismailov (2017) studies the forced vibration of the system consisting of the elastic plate, compressible viscous fluid with finite depth and rigid wall.

Note that corresponding investigations regarding the elastic, viscoelastic and piezoelectric layered systems were made in the papers by Ilhan and Koc (2015), Gao *et al.* (2016) and in many others listed and detailed in the monograph by Akbarov (2015).

There are also investigations carried out in the papers by Wu and Shih (1998), Fu *et al.* (2005), Wang *et al.* (2009) and others which relate to the dynamical response analysis of plate-fluid systems induced by a moving load. However, in these papers the fluid reaction to the plate (i.e., to the floating bridge) is taken into consideration without solution of the equations of the fluid

motion and the so-called hydrostatic force (denoted by R). This force is caused by the plate-fluid interaction is determined through the linear spring model, i.e., through the reaction $R=-kw$, where w is the vertical displacement of the plate and k is the spring constant. Consequently, in the foregoing investigations, the existence of the fluid is taken into consideration only through this spring constant and through the added mass coefficient and the approach developed therein is a very approximate one. These investigations cannot answer questions about how the fluid viscosity, fluid depth, fluid compressibility, plate thickness and moving velocity of the external force act on the “hydrostatic force” and fluid flow velocities. To find the answers to these questions it is necessary to solve the corresponding coupled fluid-plate interaction problems within the scope of the exact linearized equations described for the plate and fluid motions. Some attempts in this fields was made in the paper by Akbarov and Ismailov (2015) in which the motion of the plate is described by the exact equations of linear elastodynamics. However, the flow of the fluid is described by the linearized Navier-Stokes equations, and the dynamics of the moving load acting on the system consisting of the metal elastic plate, compressible viscous fluid and rigid wall were studied.

It should be noted that in all the foregoing papers related to the interaction of the plate and compressible viscous fluid it was assumed that the fluid is at rest. At the same time, many cases can exist in which the plate is in contact with a flowing fluid, which, as usual, is non-homogeneous, before the action of external forces, i.e., the velocities of the fluid flow depend on the space coordinates. According to this statement, the linearized Navier-Stokes equations describing the perturbation field in the fluid become equations with variable coefficients. The variability of the coefficients causes serious difficulties in obtaining an analytical solution to these equations. To prevent this difficulty, in the paper by Akbarov and Panachli (2015) a discrete-analytical solution method to these equations was developed. This method is used an analytical solution method to investigate a class of problems related to the dynamic interaction of the plate with a flowing compressible viscous fluid. Moreover, in the paper by Akbarov and Panachli (2015), convergence of the proposed method was examined and some results on the frequency response of the system under consideration are given. In the present paper, the numerical investigations which were begun in the paper by Akbarov and Panachli (2015) are continued and a lot of numerical results on the frequency response of the considered system are presented, and sufficiently-detailed analyses are made.

Note that the aforementioned discrete-analytical method was also employed in the paper by Akbarov *et al.* (2016) for investigation of the natural vibration of the three-layered solid sphere made of FGM. Moreover, we note that the study of the dynamics of the axially moving and vibrating plates are made in many investigations such as carried out in the papers by Banichuk *et al.* (2010), Yang *et al.* (2010), Yao *et al.* (2016) and other listed therein. However, in these investigations the motion of the plates are described within the scope of various approximate plate theories and rectangular plates with various edge conditions are examined.

2. Formulation of the problem and on the solution method

Consider a hydro-elastic system consisting of axially-moving elastic plate, compressible barotropic viscous fluid and rigid wall. We introduce the Cartesian coordinate system $Ox_1x_2x_3$ which is fixed on, and moves with, the plate. We also introduce the Cartesian coordinate system $O_0x_{10}x_{20}x_{30}$ which is associated with the rigid wall (Fig. 1). Considered below is the two-

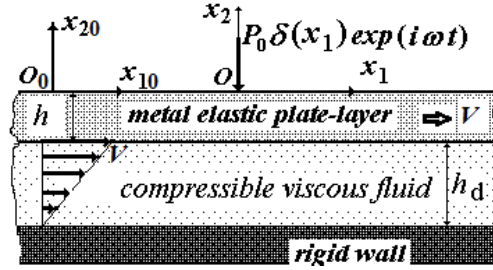


Fig. 1 Sketch of the hydro-elastic system under consideration

dimensional problem in the plane Ox_1x_2 (or in the plane $O_0x_{10}x_{20}$). Therefore, in Fig.1 the coordinate axes Ox_3 and O_0x_{30} are not shown and according to Fig. 1, the plate occupies the region $\{|x_1| < \infty, -h < x_2 < 0\}$ and the fluid occupies the region $\{|x_1| < \infty, -h_d - h < x_2 < -h\}$.

Thus we assume that the plate moves in the direction of the Ox_1 (or O_0x_{10}) axis with constant velocity V and this movement causes a corresponding flow of the fluid. According to the foregoing assumptions, there exists the following relation between the coordinates x_i and x_{i0}

$$x_1 = x_{10} - Vt, \quad x_2 = x_{20} \quad (1)$$

where t is the time.

According to Fig. 1 and the notation shown therein, we can write the following well-known expression for the fluid-flow velocity caused by the plate's axial movement.

$$v_1^0 = V \frac{x_{20}}{h_d} + V \left(\frac{h}{h_d} + 1 \right), \quad v_2^0 = 0. \quad (2)$$

Now we attempt to investigate the forced vibration of this system caused by the additional lineally-located time-harmonic forces acting on the moving plate, as shown in Fig. 1. We will assume that the amplitudes of the fluid flow velocities caused by the additional time-harmonic force are significantly less than the plate moving velocity V . Consequently, perturbation of the motion of the fluid under consideration can be described within the scope of the linearized equations. Therefore to describe this perturbation we use the linearized Navier-Stokes equations for compressible viscous fluid. However for describing the plate motion we can employ the corresponding exact equations and relations of the linear elastodynamics.

Thus, we write the complete system field equations of the linear elastodynamics in the moving system of coordinates Ox_1x_2 . These equations are

$$\begin{aligned} \frac{\partial \sigma_{11}}{\partial x_1} + \frac{\partial \sigma_{12}}{\partial x_2} = \rho \frac{\partial^2 u_1}{\partial t^2}, \quad \frac{\partial \sigma_{12}}{\partial x_1} + \frac{\partial \sigma_{22}}{\partial x_2} = \rho \frac{\partial^2 u_2}{\partial t^2}, \quad \sigma_{11} = (\lambda + 2\mu)\varepsilon_{11} + \lambda\varepsilon_{22}, \quad \sigma_{12} = 2\mu\varepsilon_{12}, \\ \sigma_{22} = \lambda\varepsilon_{11} + (\lambda + 2\mu)\varepsilon_{22}, \quad \varepsilon_{11} = \frac{\partial u_1}{\partial x_1}, \quad \varepsilon_{22} = \frac{\partial u_2}{\partial x_2}, \quad \varepsilon_{12} = \frac{1}{2} \left(\frac{\partial u_1}{\partial x_2} + \frac{\partial u_2}{\partial x_1} \right). \end{aligned} \quad (3)$$

In Eq. (3) conventional notation is used.

Now, according to Guz (2009), we write the linearized Navier-Stokes equations for the compressible viscous fluid in the fixed coordinate system $O_0x_{10}x_{20}$ (Fig. 1)

$$\begin{aligned}
 \rho_0^{(1)} \frac{\partial v_1}{\partial t} + \rho_0^{(1)} v_1^0(x_{20}) \frac{\partial v_1}{\partial x_{10}} - \mu^{(1)} \left(\frac{\partial^2 v_1}{\partial x_{10}^2} + \frac{\partial^2 v_1}{\partial x_{20}^2} \right) - (\lambda^{(1)} + \mu^{(1)}) \left(\frac{\partial^2 v_1}{\partial x_{10}^2} + \frac{\partial^2 v_2}{\partial x_{10} \partial x_{20}} \right) + \frac{\partial p^{(1)}}{\partial x_{10}} &= 0, \\
 \rho_0^{(1)} \frac{\partial v_2}{\partial t} + \rho_0^{(1)} v_1^0(x_{20}) \frac{\partial v_2}{\partial x_{10}} - \mu^{(1)} \left(\frac{\partial^2 v_2}{\partial x_{10}^2} + \frac{\partial^2 v_2}{\partial x_{20}^2} \right) - (\lambda^{(1)} + \mu^{(1)}) \left(\frac{\partial^2 v_1}{\partial x_{10} \partial x_{20}} + \frac{\partial^2 v_2}{\partial x_{20}^2} \right) + \frac{\partial p^{(1)}}{\partial x_{20}} &= 0, \\
 \frac{\partial \rho^{(1)}}{\partial t} + \rho_0^{(1)} \left(\frac{\partial v_1}{\partial x_{10}} + \frac{\partial v_2}{\partial x_{20}} \right) + v_1^0(x_{20}) \frac{\partial \rho^{(1)}}{\partial x_{10}} &= 0, \\
 T_{11} = (-p^{(1)} + \lambda^{(1)} \theta) + 2\mu^{(1)} e_{11}, \quad T_{22} = (-p^{(1)} + \lambda^{(1)} \theta) + 2\mu^{(1)} e_{22}, \quad T_{12} = 2\mu^{(1)} e_{12}, \\
 \theta = \frac{\partial v_1}{\partial x_{10}} + \frac{\partial v_2}{\partial x_{20}}, \quad e_{11} = \frac{\partial v_1}{\partial x_{10}}, \quad e_{22} = \frac{\partial v_2}{\partial x_{20}}, \\
 e_{12} = \frac{1}{2} \left(\frac{\partial v_1}{\partial x_{20}} + \frac{\partial v_2}{\partial x_{10}} \right), \quad a_0^2 = \frac{\partial p^{(1)}}{\partial \rho^{(1)}}.
 \end{aligned} \tag{4}$$

where $\rho_0^{(1)}$ is the fluid density before perturbation. The other notation used in Eq. (4) is also conventional.

Moreover, it is assumed that the following boundary, contact and impermeability conditions are satisfied

$$\begin{aligned}
 \sigma_{21}(t, x_1, x_2) \Big|_{x_2=0} &= 0, \\
 \sigma_{22}(t, x_1, x_2) \Big|_{x_2=0} &= -P_0 \delta(x_1) e^{i\omega t}, \\
 \frac{\partial u_1(t, x_1, x_2)}{\partial t} \Big|_{\substack{x_1=x_{10}-Vt \\ x_2=x_{20}=-h}} &= v_1(t, x_{10}, x_{20}) \Big|_{x_2=x_{20}=-h}, \quad \frac{\partial u_2(t, x_1, x_2)}{\partial t} \Big|_{\substack{x_1=x_{10}-Vt \\ x_2=x_{20}=-h}} = v_2(t, x_{10}, x_{20}) \Big|_{x_2=x_{20}=-h}, \\
 \sigma_{21}(t, x_1, x_2) \Big|_{\substack{x_1=x_{10}-Vt \\ x_2=x_{20}=-h}} &= T_{21}(t, x_{10}, x_{20}) \Big|_{x_2=x_{20}=-h}, \\
 \sigma_{22}(t, x_1, x_2) \Big|_{\substack{x_1=x_{10}-Vt \\ x_2=x_{20}=-h}} &= T_{22}(t, x_{10}, x_{20}) \Big|_{x_2=x_{20}=-h}, \\
 v_1(t, x_{10}, x_{20}) \Big|_{x_2=x_{20}=-h-d} &= 0, \\
 v_2(t, x_{10}, x_{20}) \Big|_{x_2=x_{20}=-h-d} &= 0.
 \end{aligned} \tag{5}$$

$$\tag{6}$$

Note that in the case where $V=0$ the foregoing formulation coincides with the corresponding one considered in the paper by Akbarov and Ismailov (2017).

This completes formulation of the problem for which the discrete-analytical method of solution was proposed in the paper by Akbarov and Panakhli (2015). Now we recall some basic steps of this method.

First, using the relations Eq. (1) and $g(x_{10}, x_{20}) = g(x_1 + Vt, x_2) = \tilde{g}(x_1, x_2)$ (the over symbol “~” will be omitted hereafter), the field equations in Eq. (4) and the contact and impermeability

conditions in Eq. (6) are rewritten in the moving coordinate system Ox_1x_2 . For this purpose the derivatives $\partial/\partial t$, $\partial/\partial x_{10}$ and $\partial/\partial x_{20}$ in Eq. (4) must be replaced with $\partial/\partial t - V\partial/\partial x_1$, $\partial/\partial x_1$ and $\partial/\partial x_2$, respectively. As a result of these replacements, we obtain the following equations instead of the equations given in Eq. (4)

$$\begin{aligned} & \rho_0^{(1)} \frac{\partial v_1}{\partial t} + \rho_0^{(1)} (v_1^0(x_2) - V) \frac{\partial v_1}{\partial x_1} - \mu^{(1)} \left(\frac{\partial^2 v_1}{\partial x_1^2} + \frac{\partial^2 v_1}{\partial x_2^2} \right) - \\ & (\lambda^{(1)} + \mu^{(1)}) \left(\frac{\partial^2 v_1}{\partial x_1^2} + \frac{\partial^2 v_2}{\partial x_1 \partial x_2} \right) + \frac{\partial p^{(1)}}{\partial x_1} = 0, \\ & \rho_0^{(1)} \frac{\partial v_2}{\partial t} + \rho_0^{(1)} (v_1^0(x_2) - V) \frac{\partial v_2}{\partial x_1} - \mu^{(1)} \left(\frac{\partial^2 v_2}{\partial x_1^2} + \frac{\partial^2 v_2}{\partial x_2^2} \right) - \\ & (\lambda^{(1)} + \mu^{(1)}) \left(\frac{\partial^2 v_1}{\partial x_1 \partial x_2} + \frac{\partial^2 v_2}{\partial x_2^2} \right) + \frac{\partial p^{(1)}}{\partial x_2} = 0, \\ & \frac{\partial \rho^{(1)}}{\partial t} + \rho_0^{(1)} \left(\frac{\partial v_1}{\partial x_1} + \frac{\partial v_2}{\partial x_2} \right) + (v_1^0(x_2) - V) \frac{\partial \rho^{(1)}}{\partial x_1} = 0, \\ & T_{11} = (-p^{(1)} + \lambda^{(1)}\theta) + 2\mu^{(1)}e_{11}, \quad T_{22} = (-p^{(1)} + \lambda^{(1)}\theta) + 2\mu^{(1)}e_{22}, \quad T_{12} = 2\mu^{(1)}e_{12}, \\ & \theta = \frac{\partial v_1}{\partial x_1} + \frac{\partial v_2}{\partial x_2}, \quad e_{11} = \frac{\partial v_1}{\partial x_1}, \quad e_{22} = \frac{\partial v_2}{\partial x_2}, \quad e_{12} = \frac{1}{2} \left(\frac{\partial v_1}{\partial x_2} + \frac{\partial v_2}{\partial x_1} \right), \quad a_0^2 = \frac{\partial p^{(1)}}{\partial \rho^{(1)}}, \end{aligned} \quad (7)$$

and the following contact and impermeability conditions instead of Eq. (6).

$$\begin{aligned} & \left. \frac{\partial u_1(t, x_1, x_2)}{\partial t} \right|_{x_2=-h} = v_1(t, x_1, x_2) \Big|_{x_2=-h}, \\ & \left. \frac{\partial u_2(t, x_1, x_2)}{\partial t} \right|_{x_2=-h} = v_2(t, x_1, x_2) \Big|_{x_2=-h}, \\ & \left. \sigma_{21}(t, x_1, x_2) \right|_{x_2=-h} = T_{21}(t, x_1, x_2) \Big|_{x_2=-h}, \\ & \left. \sigma_{22}(t, x_1, x_2) \right|_{x_2=-h} = T_{22}(t, x_1, x_2) \Big|_{x_2=-h}, \\ & v_1(t, x_1, x_2) \Big|_{x_2=-h-h_d} = 0, \\ & v_2(t, x_1, x_2) \Big|_{x_2=-h-h_d} = 0 \end{aligned} \quad (8)$$

In this way, we have all the field equations and relations in the moving system of coordinates Ox_1x_2 and, according to the boundary condition Eq. (5), we can represent all sought quantities as $d(t, x_1, x_2) = \bar{d}(x_1, x_2)e^{i\omega t}$ (the over-bar will be omitted below) in this coordinate system. Substituting this into the foregoing equations and conditions, we obtain the corresponding equations and relations for the amplitudes of the sought values. Moreover, after this procedure we apply the

exponential Fourier transformation

$$f_F(s, x_2) = \int_{-\infty}^{+\infty} f(x_1, x_2) e^{-isx_1} dx_1 \tag{9}$$

to the foregoing equations and relations. As a result, we obtain the field equations and relations for the Fourier transformations of the sought values. It should be noted that finding the analytical expression for the values related to the plate does not have any serious difficulties. However, to find the analytical solution to the system of equations obtained from the Eq. (7) after the Fourier transformation is not so simple because this system contains the variable coefficient $V_1^0(x_2)$ ($=v_1^0(x_2) - V$). Therefore, in the paper by Akbarov and Panachli (2015) the discrete-analytical solution method was proposed to solve this system of equations, the essence of which is as follows:

The strip $S = [-h_d - h \leq x_2 \leq -h]$ which is filled with the fluid is divided into the following M sub-strips

$$S_k = \left[-k \frac{h_d}{M} - h \leq x_2 \leq -(k-1) \frac{h_d}{M} - h \right], \quad k = 1, 2, \dots, M, \quad S = \sum_{k=1}^M S_k \tag{10}$$

and it is assumed that in each of these strips, the function $V_1^0(x_2)$ is constant and equal to

$$V_1^{0(k)} = V_1^0(x_2) \Big|_{x_2 = -h - (2k-1)h_d/(2M)}. \tag{11}$$

Taking the relations (10) and (11) into consideration, it is supposed that the system of equations in Eq. (7) is satisfied separately within each strip S_k . So that within each strip we obtain the corresponding field equations with their corresponding constant coefficients. Moreover, contact conditions on the interface between the strip S_1 and plate, on the interfaces between the strips S_1, \dots, S_M Eq. (10) and on the interface between the strip S_M and the rigid wall are derived from the continuity assumption. To find the solution of the field equations in each strip, the general solution presentation proposed by Guz (2009) is used. In this way the analytical expression for the Fourier transformation of the sought values related to the fluid flow is determined. Under this determination procedure

the following notation is introduced

$$\begin{aligned} \Omega_1^{(k)} &= \frac{\omega h}{a_0} + \frac{hsV_1^{(k)}}{a_0} = \Omega_{10} + \Omega_{11} sh \left(\frac{x_2}{h_d} + \frac{h}{h_d} \right) \Big|_{x_2 = -h - (2k-1)h_d/(2M)}, \\ \Omega_{10} &= \frac{\omega h}{a_0}, \quad \Omega_{11} = \frac{V}{a_0}, \quad N_w^{(k)2} = \frac{\omega h^2}{\nu^{(1)}} + \frac{Vh}{\nu^{(1)}} sh \left(\frac{x_2}{h_d} + \frac{h}{h_d} \right) \Big|_{x_2 = -h - (2k-1)h_d/(2M)} = \\ N_{w0}^2 + N_{w1}^2 sh \left(\frac{x_2}{h_d} + \frac{h}{h_d} \right) \Big|_{x_2 = -h - (2k-1)h_d/(2M)}, \quad N_{w0}^2 &= \frac{\omega h^2}{\nu^{(1)}}, \quad N_{w1}^2 = \frac{Vh}{\nu^{(1)}}. \end{aligned} \tag{12}$$

The dimensionless parameters N_{w0} and N_{w1} in Eq. (12) can be taken as the parameters which characterizes the influence of the fluid viscosity on the mechanical behavior of the system. At the same time, the dimensionless parameters Ω_{10} and Ω_{11} in Eq. (12) can be taken as the parameter

which characterizes the influence of the compressibility of the fluid on the mechanical behavior of the system.

In this way the Fourier transformation of the sought quantities is determined completely, after which these quantities are found from the inverse transformation.

$$\left\{ \sigma_{22}, \sigma_{11}, u_1, u_2, T_{22}^{(k)}, T_{11}^{(k)}, T_{12}^{(k)}, v_1^{(k)}, v_2^{(k)} \right\} = \frac{1}{2\pi} \operatorname{Re} \left\{ e^{i\omega t} \int_{-\infty}^{+\infty} [\sigma_{22F}, \sigma_{11F}, u_{1F}, u_{2F}, T_{22F}^{(k)}, T_{11F}^{(k)}, T_{12F}^{(k)}, v_{1F}^{(k)}, v_{2F}^{(k)}] e^{isx_1} ds \right\} \quad (13)$$

It should be noted that under the foregoing solution procedure the number M is determined from the convergence requirement of the numerical results obtained from the calculation of the integrals in Eq. (13). Note that examples to verify the method discussed briefly above are given in a detail in the paper by Akbarov and Panakhli (2015). In this paper it is also shown that for the cases which will be considered below in order to obtain the numerical results with high accurate and convergence it is enough to assume that $M=15$ in Eq. (10). Therefore, we do not consider here these examples again because this would be a repetition of those which were given already in the previous paper by authors.

Consequently, the paper Akbarov and Panakhli (2015) relates namely to the development of the aforementioned solution method and to test this method on some regarding examples. However, the present paper relates to the detail consideration and analyses of the numerical results obtained with use the method developed in the previous paper by authors. Namely this is the difference between the present and previous papers by authors.

3. Numerical results and discussions

We assume that the material of the plate-layer is Steel with mechanical constants: $\mu=79 \times 10^9$ Pa, $\lambda=94.4 \times 10^9$ Pa and density $\rho=7790$ kg/m³ (Guz and Makhort 2000, Guz 2004), but the material of the fluid is Glycerin with viscosity coefficient $\mu^{(1)}=1.393$ kg/(m·s), density $\rho_0=1260$ kg/m³ and sound speed $a_0=1927$ m/s (Guz 2009). We also introduce the notation $c_2 = \sqrt{\mu/\rho}$ which is the shear wave propagation velocity in the plate material. After selection of these materials, the dimensionless parameters such as Ω_{10} , Ω_{11} , N_{w0} and N_{w1} in Eq. (12) and dimensionless parameter $M_\omega (= \mu^{(1)}\omega/\mu)$ which arises in contact conditions between the S_1 fluid sub-strip and the plate, can be determined through the four quantities: h (the thickness of the plate-layer), h_d (the thickness of the fluid strip), V (the plate's axial moving velocity) and ω (the frequency of the time-harmonic external forces). At the same time, it should be noted that it can be elected directly the values for the foregoing dimensionless problem parameters without selecting the values for the parameters h , h_d , V and ω , and investigate frequency responses of the related quantities. However, under investigations with the use of the aforementioned dimensionless parameters many difficulties related to the reality of the selected values appear and this statement confuse the analyses, explanation and understanding of the obtained numerical results. However, determination of the values of the dimensionless parameters through the selected values of the h , h_d , V and ω , and

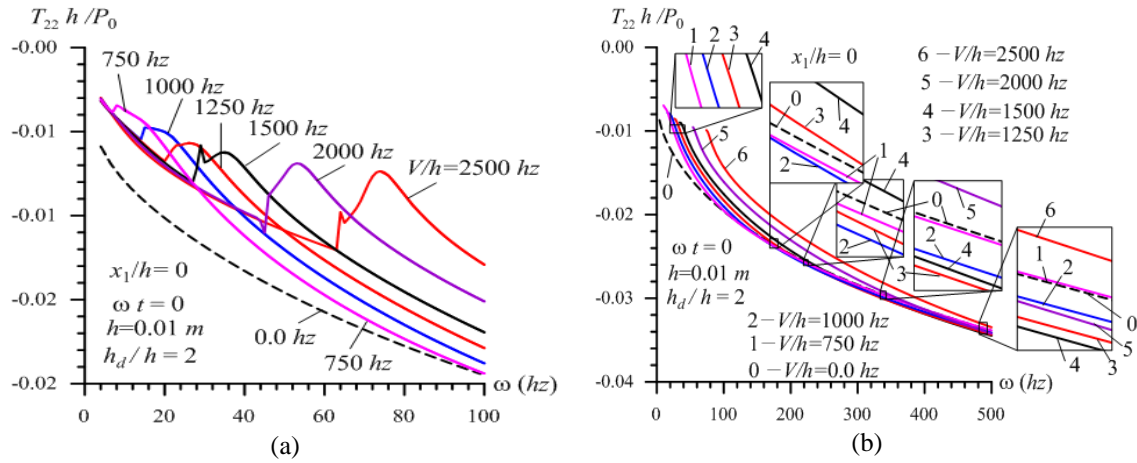


Fig. 2 The influence of the plate moving velocity on the frequency response of the dimensionless stress $T_{22}h/P_0$ in the cases where $4\text{ hz} \leq \omega \leq 100\text{ hz}$ (a) and $\omega_{cr} < \omega' \leq \omega \leq 500\text{ hz}$ (b)

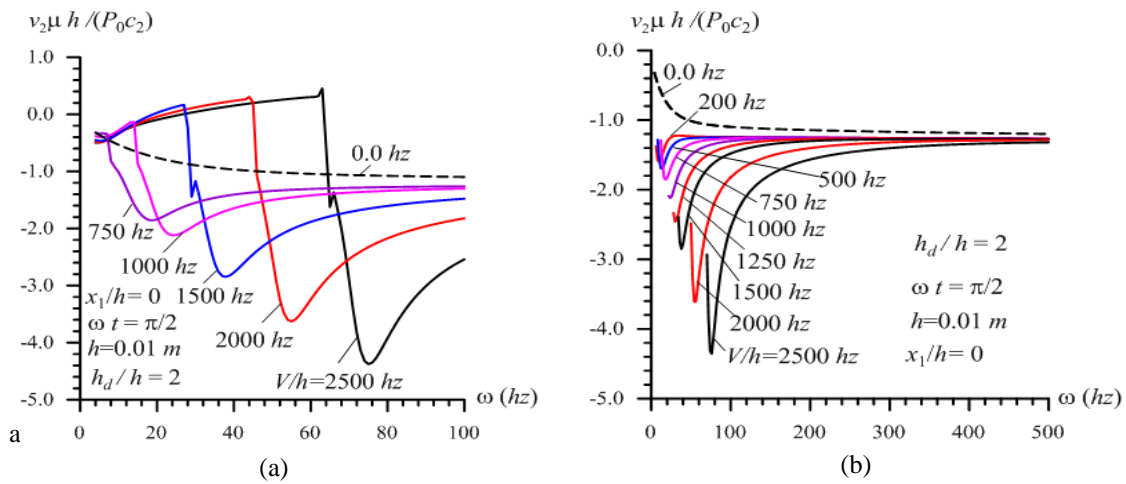


Fig. 3 The influence of the plate moving velocity on the frequency response of the dimensionless velocity $v_2\mu h/(P_0c_2)$ in the cases where $4\text{ hz} \leq \omega \leq 100\text{ hz}$ (a) and $\omega_{cr} < \omega' \leq \omega \leq 500\text{ hz}$ (b)

analyses of the numerical results with respect to values of these dimensional parameters gives clear presentation on the obtained numerical results. Therefore, in the present investigation we select the latter form analyses, i.e., analyses through the values of the parameters h , h_d , V and ω , among which the main parameter for the present investigation is the plate moving velocity V in the initial state. As a result of this moving velocity, all solution difficulties and new mechanical effects appear, as will be discussed below. Therefore, in all the numerical investigations the focus is on the influence of the moving velocity V on the frequency response of the hydro-elastic system under consideration.

Before discussion of the numerical results, we note that under calculation procedures, the improper integral $\int_{-\infty}^{+\infty} f(s)e^{isx_1}ds$ in Eq. (13) is replaced by the corresponding definite integrals

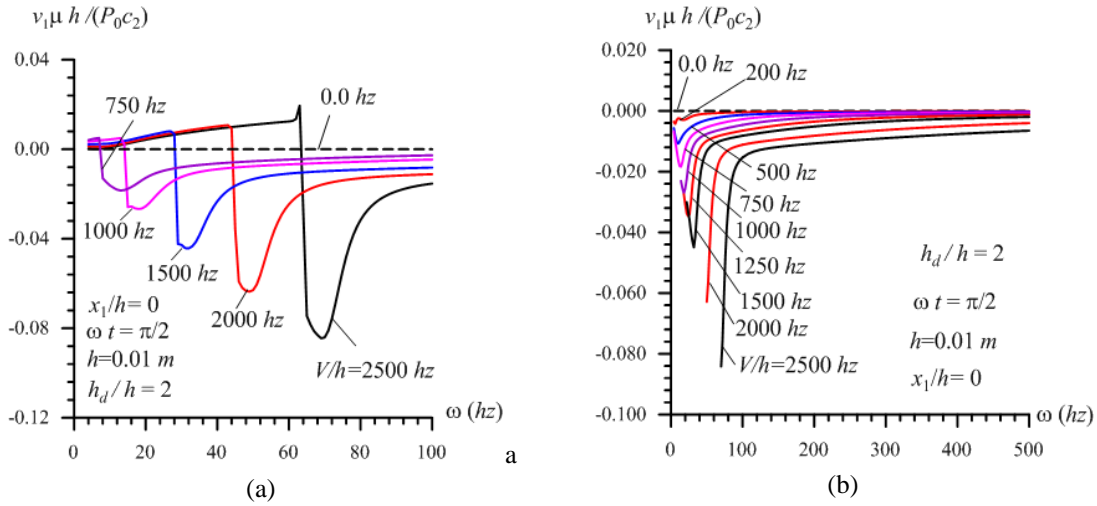


Fig. 4 The influence of the plate moving velocity on the frequency response of the dimensionless velocity $v_1\mu h/(P_0c_2)$ in the cases where $4\text{ hz} \leq \omega \leq 100\text{ hz}$ (a) and $\omega_{cr} < \omega' \leq \omega \leq 500\text{ hz}$ (b)

$\int_{-S_1^*}^{+S_1^*} f(s)e^{isx_1} ds$. The values of S_1^* are determined from the convergence requirement of the numerical results. Note that under calculation of the integral $\int_{-S_1^*}^{+S_1^*} f(s)e^{isx_1} ds$, the integration interval $[-S_1^*; +S_1^*]$ is further divided into a certain number (denote it by N) of shorter intervals, which are used in the Gauss integration algorithm. The values of the integrated expressions at the sample points are calculated through the solution procedures of the corresponding boundary-contact value problems. All procedures were performed automatically with the PC programs constructed by the authors in MATLAB.

Convergence of the numerical results with respect to the parameters M , N and S_1^* was discussed in the paper by Akbarov and Panakhli (2015) and therefore here we do not consider it again. Nevertheless, we note that all numerical results, which will be discussed below, are obtained in the case where $M=15$, $N=2000$ and $S_1^* = 5$.

3.1 The influence of the plate moving velocity, plate thickness and fluid depth on the frequency response of the stress and velocities and on the critical frequencies

According to the paper by Akbarov and Panakhli (2015), we recall that under the critical frequency we will understand the frequency under which the amplitude of the studied quantities has a jump. Thus, after this recalling, first, we consider the influence of the plate moving velocity V on the frequency response of the normal stress and velocities arising on the interface plane between the plate and fluid. The graphs given in Figs. 2, 3 and 4 show the dependence among the dimensionless stress $T_{22}h/P_0$ (Fig. 2 under $\omega t=0$), the dimensionless velocity $v_2\mu h/(P_0c_2)$ (Fig. 3 under $\omega t=\pi/2$), the dimensionless velocity $v_1\mu h/(P_0c_2)$ (Fig. 4 under $\omega t=\pi/2$) and the frequency ω which are constructed for various values of V/h in the case where $h_d/h=2$, and $x_1/h=0$. Note that for

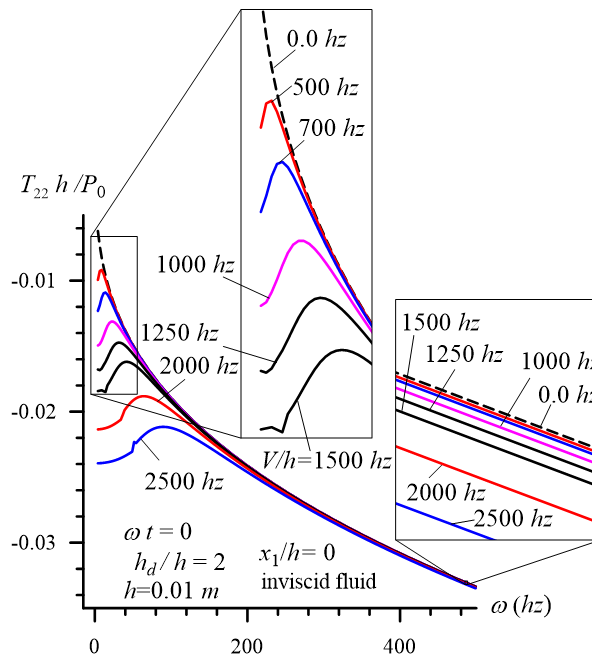


Fig. 5 The influence of the plate moving velocity on the frequency response of the dimensionless stress $T_{22}h/P_0$ in the case where the fluid is modeled as inviscid

a clear illustration of the influence of the moving plate velocity on the values of the critical frequency as well as on the values of the studied quantities the graphs related to the cases where $4\text{ hz} \leq \omega \leq 100$ and $\omega_{cr} < \omega' \leq \omega \leq 500 \text{ hz}$ are presented separately by letters *a* and *b*, respectively. Here the values of ω' vary according to V/h and these values can be easily determined from the foregoing figures. Moreover, note that in these figures the dashed lines show the frequency response of the corresponding quantity in the case where the plate in the initial state is at rest, i.e., the case where $V/h=0$ and here and below the results illustrated with these dashed lines coincide with corresponding ones obtained in the paper by Akbarov and Ismailov (2017).

Thus, it follows from the results given in Figs. 2-4 that the values of ω_{cr} decrease with decreasing plate axial-moving velocity V/h . Moreover the graphs show that there exists a certain value of the frequency (denoted by ω^*) before which (i.e., for $\omega' < \omega < \omega^*$) the plate moving velocity in the initial state causes a decrease (an increase) in the absolute values of the dimensionless stress $T_{22}h/P_0$ (of the dimensionless velocities $v_2\mu h/(P_0c_2)$ and $v_1\mu h/(P_0c_2)$) with respect to the corresponding ones obtained in the case where $V/h=0$. However, after this frequency (i.e., in the cases where $\omega > \omega^*$) the plate moving velocity causes the absolute values of $T_{22}h/P_0$ with respect to those obtained in the case where $V/h=0$ to increase slightly.

To demonstrate the influence of the fluid viscosity on the values of the studied quantities, graphs of the frequency response of the dimensionless stress $T_{22}h/P_0$ in the case where the fluid is modelled as inviscid are given in Fig. 5. Comparison of these graphs with the corresponding ones given in Fig. 2 shows that the influence of the fluid viscosity on the studied frequency response has important significance, not only qualitatively but also quantitatively. We recall that in the case where the plate is in contact with the inviscid fluid, the plate moving in the initial state does not cause the fluid flow. Consequently, the inviscid fluid model is not adequate for mathematical

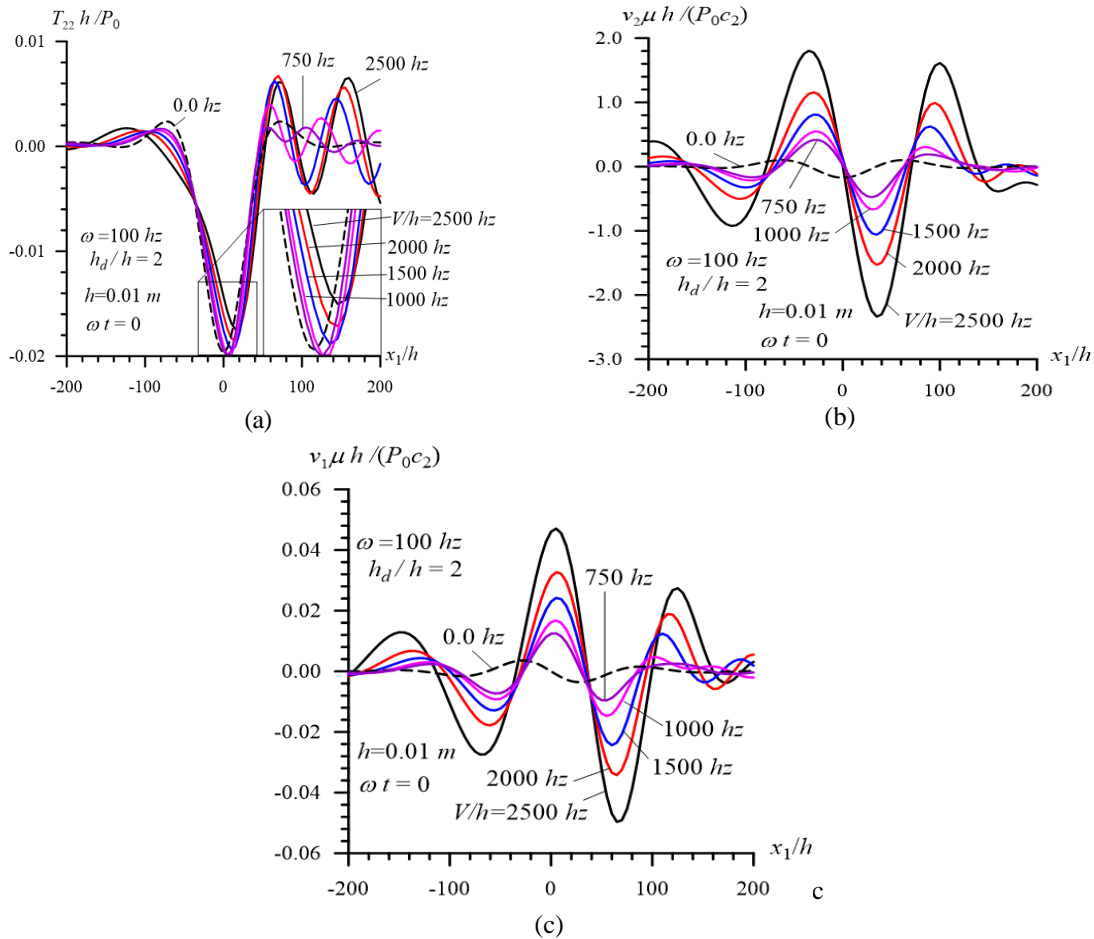


Fig. 6 The influence of the plate moving velocity on the distribution of $T_{22}h/P_0$ (a), $v_2\mu h/(P_0c_2)$ (b) and $v_1\mu h/(P_0c_2)$ (c) with respect to x_1/h

modelling of the type of problems studied. This result shows again the significance of the proposed approach for solution to the dynamic problems related to hydro-elastic systems containing a viscous fluid.

Note that the results illustrated in Figs. 3-5 were also given in the paper by Akbarov and Panachli (2015). Nevertheless, for readability and for compact illustration of the related results and for their comparison with each other we give again these results here.

Another characteristic of the influence of the plate's axially-moving velocity on the plate-fluid interaction under consideration is illustrated in the case where $V/h=0$ and detailed in the paper by Akbarov and Ismailov (2017), i.e., in the case where the plate is at rest in the initial state and the distribution of the stresses and velocities caused by the additional time harmonic forces with respect to the moving coordinate x_1/h is symmetric or asymmetric with respect to the point $x_1/h=0$. However, as can be predicted according to expressions and Eqs. (21)-(25), in the case where $V/h>0$ this distribution becomes non-symmetric or non-asymmetric with respect to $x_1/h=0$, i.e., with respect to the point at which the external additional time-harmonic force acts. The results that

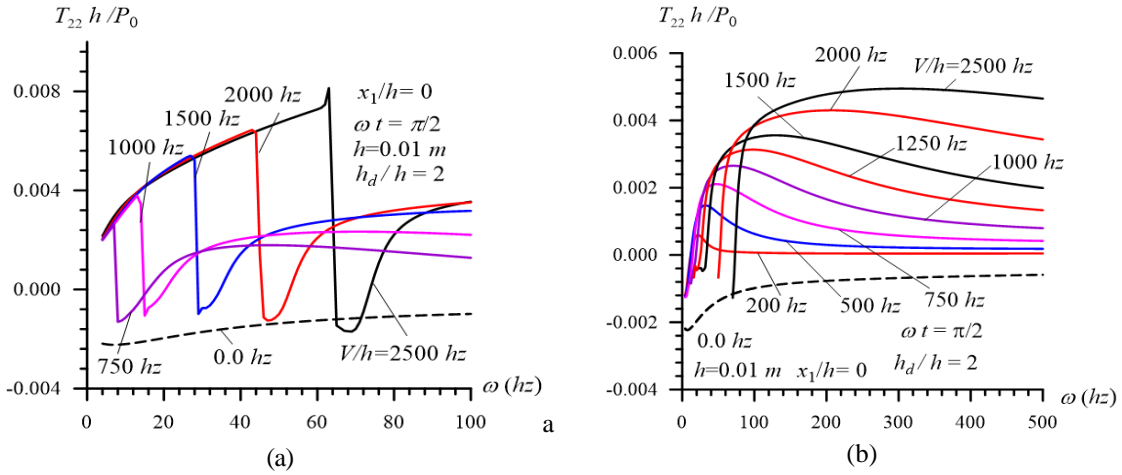


Fig. 7 Frequency response of $T_{22}h/P_0$ under $h=0.01m$, $h_d/h=2$, $\omega t = \pi/2$ and $x_1/h=0$ for various values of the plate moving velocity V/h in the cases where $4hz \leq \omega \leq 100hz$ (a) and $\omega_{cr} < \omega' \leq \omega \leq 500hz$ (b)

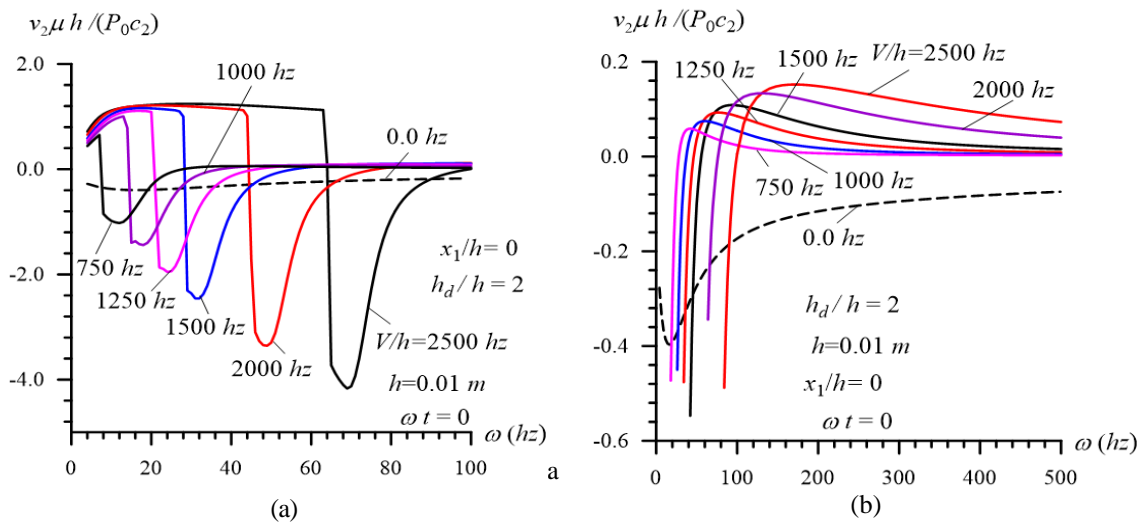


Fig. 8 Frequency response of $v_2\mu h/(P_0c_2)$ under $h=0.01m$, $h_d/h=2$, $\omega t=0$ and $x_1/h=0$ for various values of the plate moving velocity V/h in the cases where $4hz \leq \omega \leq 100hz$ (a) and $\omega_{cr} < \omega' \leq \omega \leq 500hz$ (b)

prove this conclusion are illustrated in the graphs in Fig. 6 which show the distribution for the dimensionless stress $T_{22}h/P_0$ (Fig. 6(a)) and velocities $v_2\mu h/(P_0c_2)$ (Fig. 6(b)) and $v_1\mu h/(P_0c_2)$ (Fig. 6(c)) in the case where $\omega=100hz$ and $\omega t=0$.

We continue the aforementioned investigations and consider the graphs given in Figs. 7, 8 and 9 which show the frequency response of $T_{22}h/P_0$ (Fig. 7) under $\omega t=\pi/2$ and velocities $v_2\mu h/(P_0c_2)$ (Fig. 8) and $v_1\mu h/(P_0c_2)$ (Fig. 9) under $\omega t=0$, calculated at point $x_1/h=0$ in the case where $h_d/h=2$

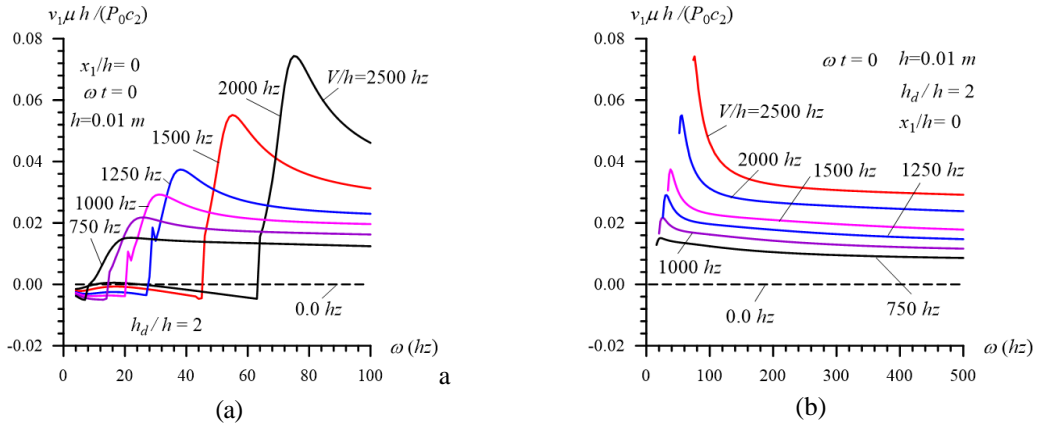


Fig. 9 Frequency response of $v_1 \mu h / (P_0 c_2)$ under $h = 0.01 \text{ m}$, $h_d/h = 2$, $\omega t = 0$ and $x_1/h = 0$ for various values of the plate moving velocity V/h in the cases where $4 \text{ Hz} \leq \omega \leq 100 \text{ Hz}$ (a) and $\omega_{cr} < \omega' \leq \omega \leq 500 \text{ Hz}$ (b)

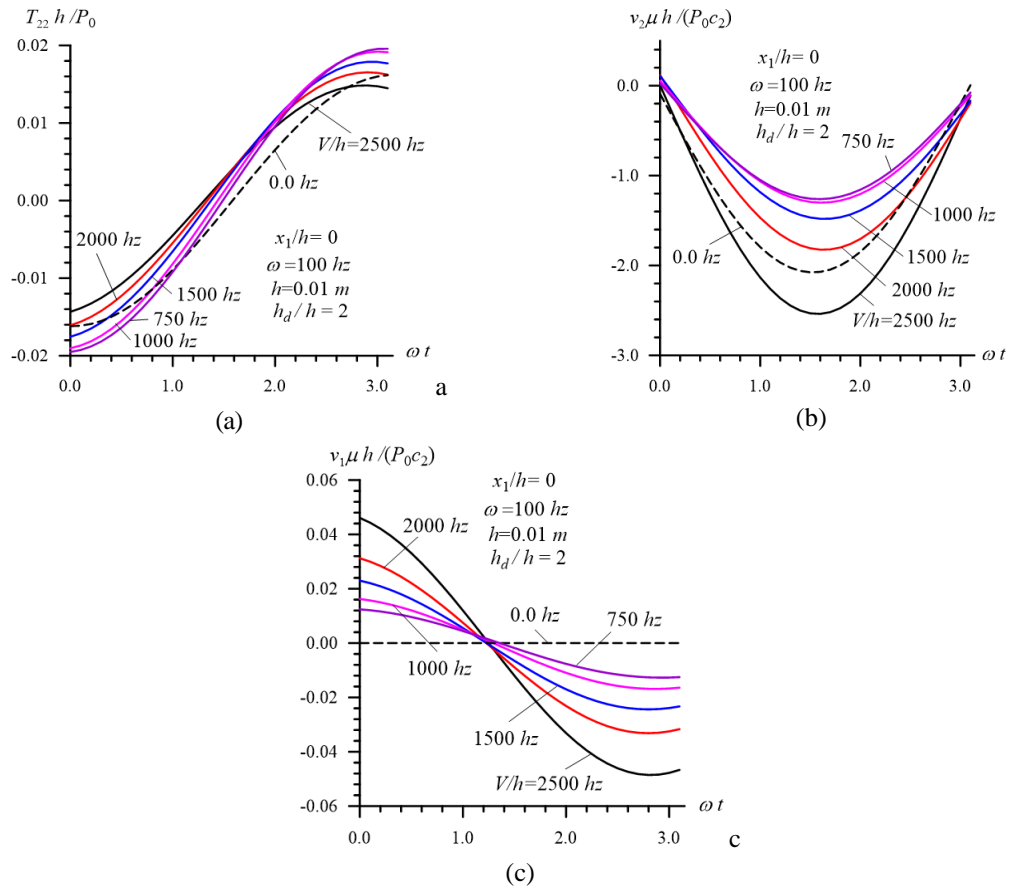


Fig. 10 Dependence of $T_{22} h / P_0$ (a), $v_2 \mu h / (P_0 c_2)$ (b) and $v_1 \mu h / (P_0 c_2)$ (c) on the frequency phase ωt for various values of the plate moving velocity V/h under $\omega = 100 \text{ Hz}$, $h = 0.01 \text{ m}$, $h_d/h = 2$ and $x_1/h = 0$

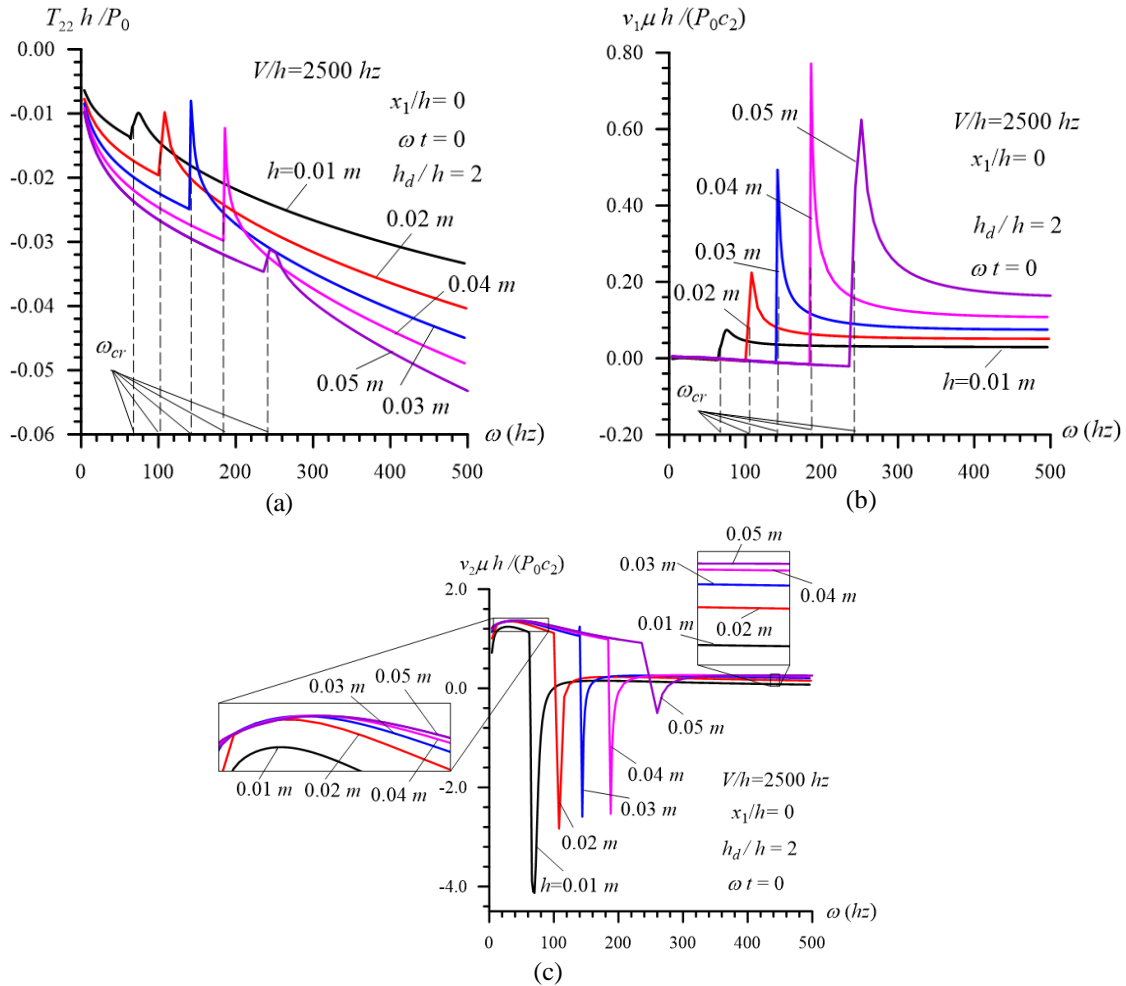


Fig. 11 The influence of the plate thickness h on the frequency response of $T_{22}h/P_0$ (a), $v_1\mu h/(P_0c_2)$ (b) and $v_3\mu h/(P_0c_2)$ (c), and on the critical frequency ω_{cr} in the case where $V/h=2500\text{ hz}$, $\omega t=0$, $h_d/h=2$ and $x_1/h=0$

and $h=0.01\text{ m}$ under $4\text{ hz} \leq \omega \leq 500\text{ hz}$. In order to clearly demonstrate the existence of the critical frequencies and the values of these frequencies, i.e., the values of ω_{cr} , in these figures the graphs grouped by the letter a are constructed in the case where $4\text{ hz} \leq \omega \leq 500\text{ hz}$ and the graphs grouped by the letter b are constructed in the case where $\omega_{cr} < \omega' \leq 500\text{ hz}$. Comparison of the graphs given in Figs. 7, 8 and 9 with the corresponding ones given in Figs. 2, 3 and 4 shows that the values of the stress and velocities depend significantly on the vibration phase ωt . It should be noted that the plate moving velocity can act significantly on the influence of the vibration phase ωt on the values of the stress and velocities. The graphs given in Fig. 10 which illustrate dependencies among $T_{22}h/P_0$ (Fig. 10(a)), $v_2\mu h/(P_0c_2)$ (Fig. 10(b)), $v_1\mu h/(P_0c_2)$ (Fig. 10(c)) and ωt for various values of the plate moving velocity V/h in the case where $\omega=100\text{ hz}$, $x_1/h=0$, $h=0.01\text{ m}$ and $h_d/h=2$, are evidence of the foregoing conclusion.

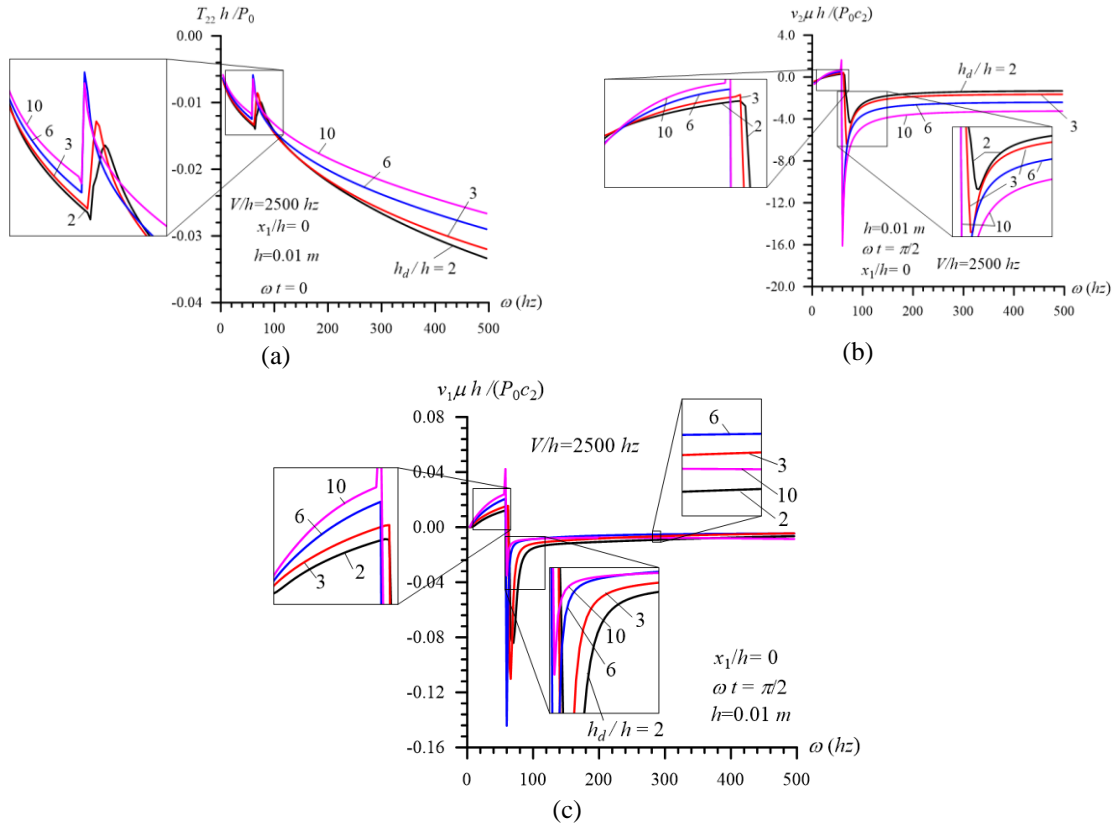


Fig. 12 The influence of the fluid depth h_d/h on the frequency response of $T_{22}h/P_0$ (a), $v_2\mu h/(P_0c_2)$ (b) and $v_1\mu h/(P_0c_2)$ (c), and on the critical frequency ω_{cr} in the case where $V/h = 2500 \text{ hz}$, $\omega t = 0$, $h = 0.01 \text{ m}$ and $x_1/h = 0$

Consider the graphs given in Fig. 11 which show the frequency response of $T_{22}h/P_0$ (Fig. 11(a)), $v_2\mu h/(P_0c_2)$ (Fig. 11(b)) and $v_1\mu h/(P_0c_2)$ (Fig. 11(c)) for various plate thickness h in the case where $x_1/h=0$, $\omega t=0$, $h_d/h=2$ and $V/h=2500 \text{ hz}$. It follows from these graphs that the values of the critical frequency ω_{cr} increase with the plate thickness.

It should be noted that under construction of these and other graphs considered in the present paper, for clarity of the illustrations, the part of the graphs corresponding to the vicinity of the critical frequency, i.e., the part which corresponds to the interval $[\omega_{cr}-\delta, \omega_{cr}+\delta]$ is omitted and the values of the studied quantities obtained at $\omega_{cr}-\delta$ and at $\omega_{cr}+\delta$ are connected with each other by a straight line.

The graphs given in Fig. 12 show the influence of the fluid depth on the values of the critical frequency ω_{cr} and on the frequency response of $T_{22}h/P_0$ (Fig. 12(a), under $\omega t=0$), $v_2\mu h/(P_0c_2)$ (Fig. 12(b), under $\omega t=\pi/2$) and $v_1\mu h/(P_0c_2)$ (Fig. 12(c), under $\omega t=\pi/2$) in the case where $h=0.01 \text{ m}$, $x_1/h=0$ and $V/h=2500 \text{ hz}$. According to these graphs, it can be concluded that an increase in the values of h_d/h causes an insignificant decrease in the values of ω_{cr} .

Consider also the frequency response of the studied quantities for the relatively thick plate and analyze the influence of the plate moving velocity on the critical velocity. Graphs of these

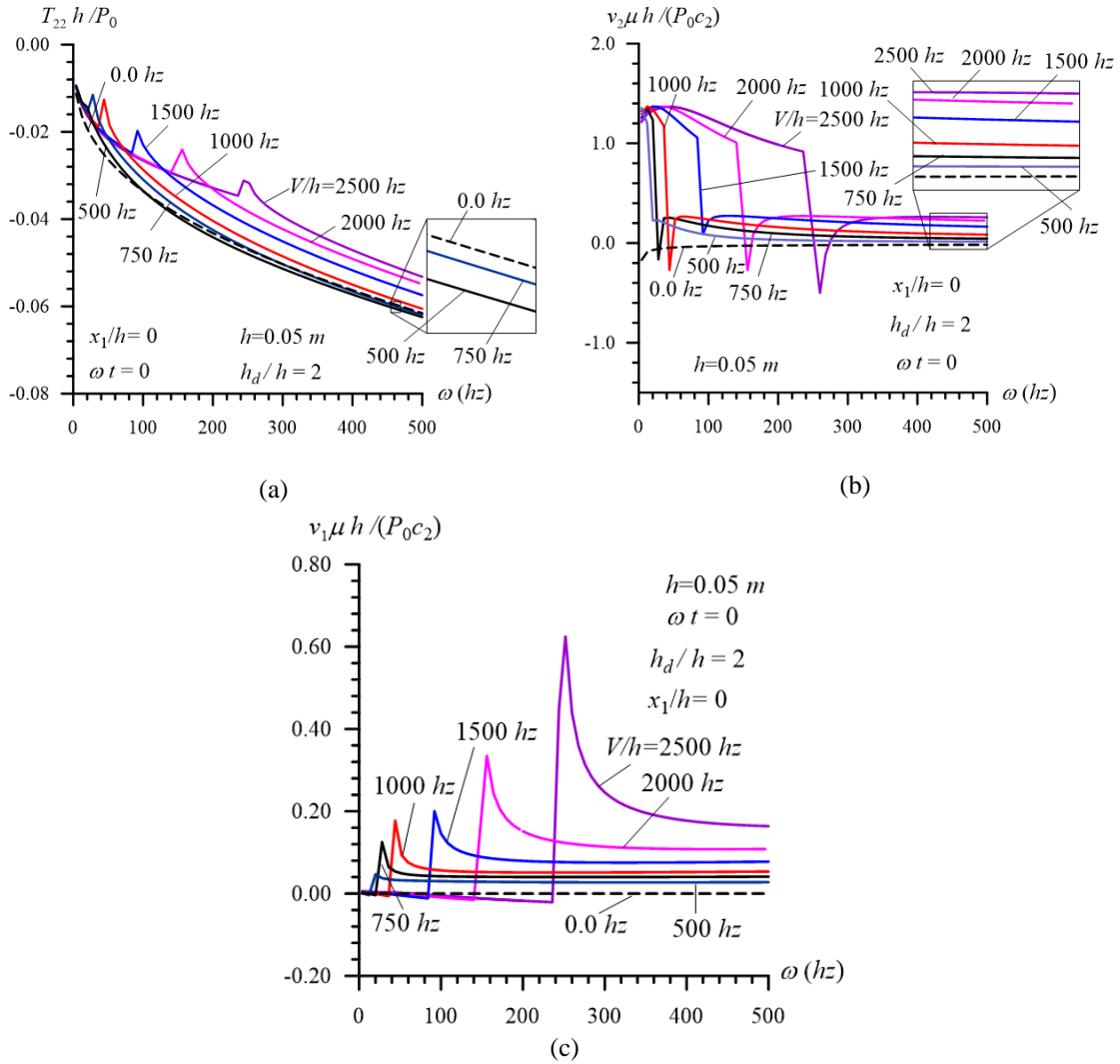


Fig. 13 Frequency response of $T_{22}h/P_0$ (a), $v_2\mu h/(P_0c_2)$ (b) and $v_1\mu h/(P_0c_2)$ (c) and critical frequencies ω_{CR} for various values of V/h in the case where $h=0.05\text{ m}$, $\omega t=0$, $h_d/h=2$ and $x_1/h=0$

responses are given in Fig. 13 which correspond to the dependencies among $T_{22}h/P_0$ (Fig. 13(a)), $v_2\mu h/(P_0c_2)$ (Fig. 13(b)), $v_1\mu h/(P_0c_2)$ (Fig. 13(c)) and ω for various values of V/h in the case where $\omega t=0$, $x_1/h=0$, $h_d/h=2$ and $h=0.05\text{ m}$. It follows from the graphs, that in the relatively thick plate case, the influence of the plate moving velocity on the critical velocity is more considerable and, as in the case where $h=0.01\text{ m}$, an increase in the values of V/h causes an increase in the values of the critical velocity.

Numerical investigations show that in the large change range of the frequency ω within the scope of certain conditions, after the first critical frequency which has been discussed above, the second critical frequency also appears. For illustration of these results we continue consideration of the frequency response of the studied quantities for the relatively thick plate, i.e., for $h=0.05$,

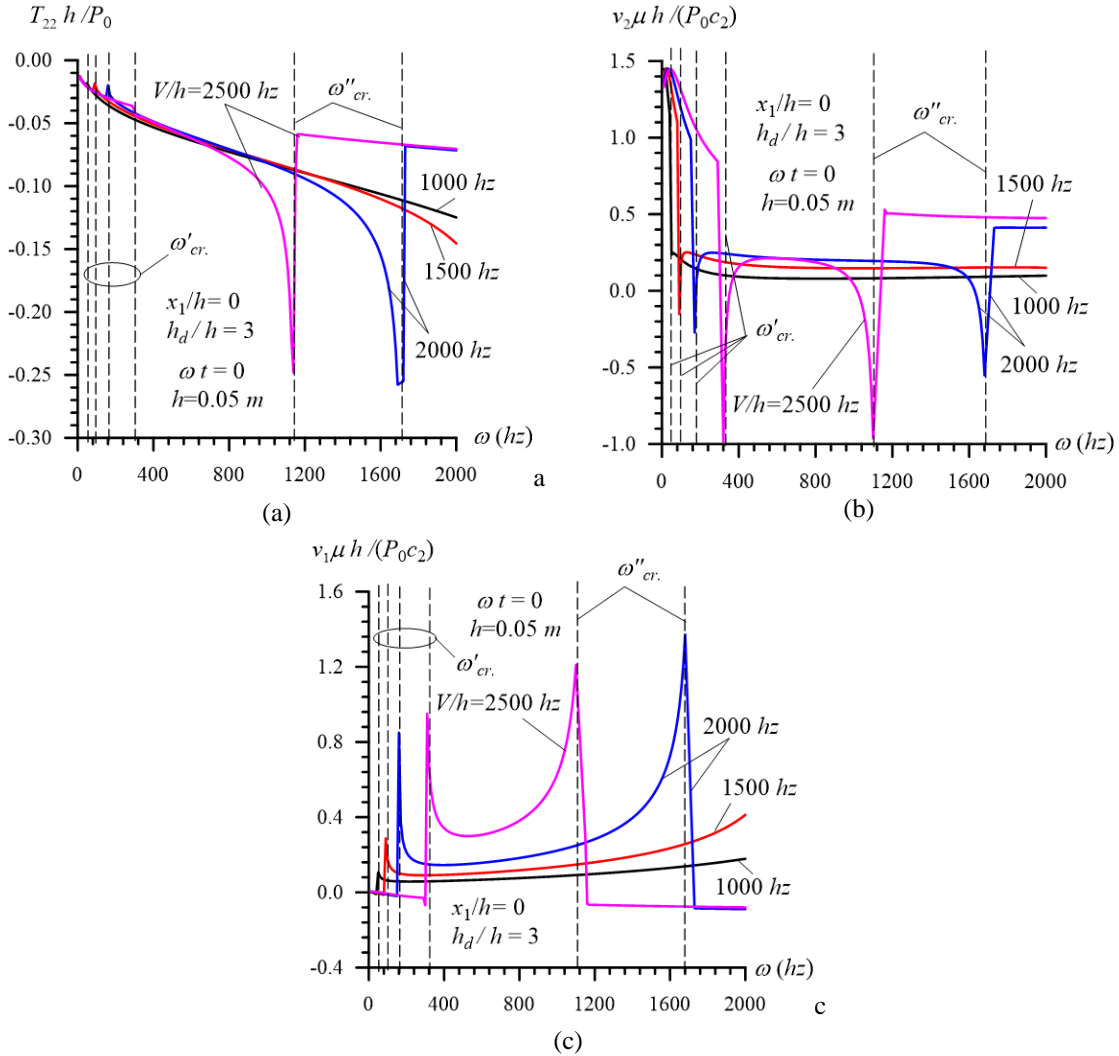


Fig. 14 Frequency response of $T_{22}h/P_0$ (a), $v_2\mu h/(P_0c_2)$ (b) and $v_1\mu h/(P_0c_2)$ (c) and critical frequencies ω'_{cr} and ω''_{cr} for various values of V/h in the case where $h=0.05$ m, $\omega t=0$, $h_d/h=2$ and $x_1/h=0$ under $4\text{ Hz} \leq \omega \leq 2000\text{ Hz}$

0.06 and 0.07 in the case where $4\text{ Hz} \leq \omega \leq 2000\text{ Hz}$ (for $h=0.05$) and $4\text{ Hz} \leq \omega \leq 1500\text{ Hz}$ (for $h=0.06$ and 0.07 m). Graphs of these responses, constructed for $1000\text{ Hz} \leq V/h \leq 2500\text{ Hz}$ under $\omega t=0$, $x_1/h=0$ and $h_d/h=3$ are given in Figs. 14 (for $h=0.05$), 15 (for $h=0.06$) and 16 (for $h=0.07$). In these figures the graphs grouped by the letters a, b and c correspond to the dimensionless stress $T_{22}h/P_0$ and dimensionless velocities $v_2\mu h/(P_0c_2)$ and $v_1\mu h/(P_0c_2)$, respectively. According to Figs. 14, 15 and 16, we introduce the notation ω'_{cr} and ω''_{cr} to indicate the first and second critical frequencies.

Thus, it follows from these figures that the values of ω'_{cr} increase, but the values of the ω''_{cr} decrease with the plate moving velocity V/h and there exists such a limit value of V/h (denote it by V^*/h) after which, i.e., in the cases where $V/h > V^*/h$, the critical frequencies disappear. Note that in

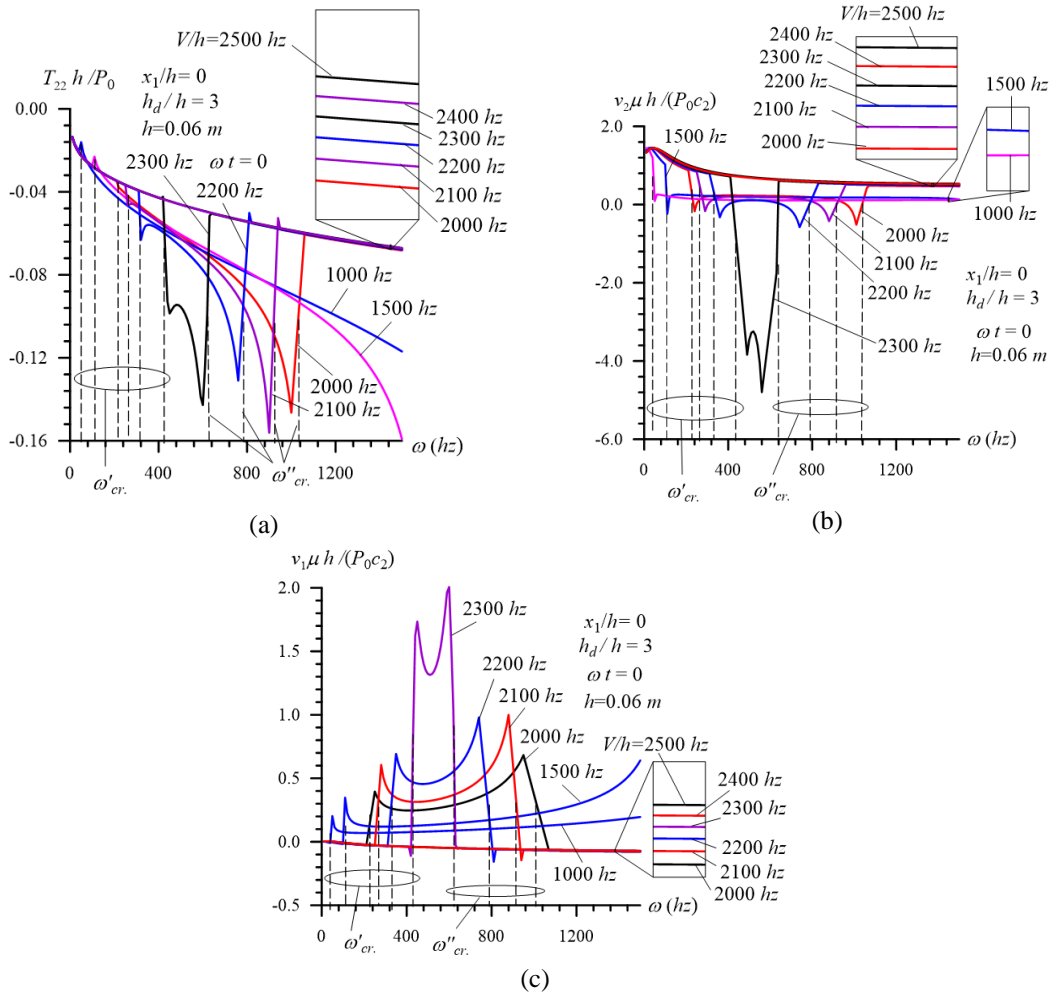


Fig. 15 Frequency response of $T_{22}h/P_0$ (a), $v_2\mu h/(P_0c_2)$ (b) and $v_1\mu h/(P_0c_2)$ (c) and critical frequencies ω'_{cr} and ω''_{cr} for various values of V/h in the case where $h=0.06m$, $\omega t=0$, $h_d/h=2$ and $x_1/h=0$ under $4hz \leq \omega \leq 1500hz$

Fig. 14, i.e., in the case where $h=0.05$ within the scope of the considered change range of V/h , the limit velocity V^*/h does not exist. However, it follows from Figs. 15 and 16 that in the cases where $h=0.06$ and $h=0.07$, the limit values of the plate moving velocity V^*/h are determined as 2300 Hz and 1950 Hz , respectively. Consequently, the values of V^*/h decrease with the plate thickness h .

We recall that, as above, under construction of the graphs given in Figs. 14, 15 and 16, for clarity of the illustrations, the parts of the graphs corresponding to the vicinity of the critical frequencies, i.e., the parts which corresponds to the interval $[\omega'_{cr}-\delta, \omega'_{cr}+\delta]$ and $[\omega''_{cr}-\delta, \omega''_{cr}+\delta]$ are omitted and the values of the studied quantities obtained at $\omega'_{cr}-\delta$ and at $\omega'_{cr}+\delta$, as well as at $\omega''_{cr}-\delta$ and at $\omega''_{cr}+\delta$ are connected with each other by the corresponding straight lines.

All the numerical results discussed above are calculated at the point $x_1/h=0$. Examples of the numerical results related to the distribution of the studied quantities with respect to the coordinate

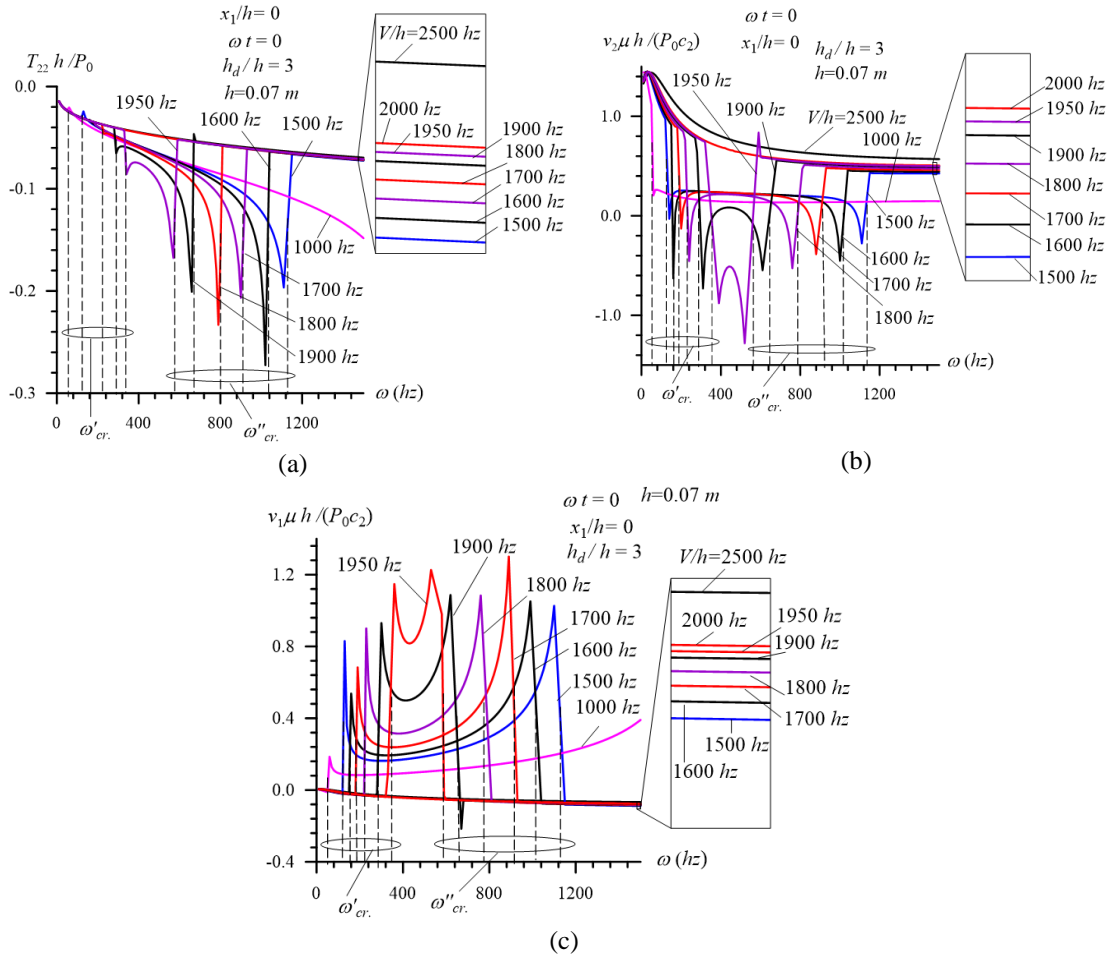


Fig. 16 Frequency response of $T_{22}h/P_0$ (a), $v_2\mu h/(P_0c_2)$ (b) and $v_1\mu h/(P_0c_2)$ (c) and critical frequencies ω'_{cr} and ω''_{cr} for various values of V/h in the case where $h = 0.07$ m, $\omega t = 0$, $h_d/h = 2$ and $x_1/h = 0$ under $4\text{ Hz} \leq \omega \leq 1500\text{ Hz}$

x_1/h are given in Fig. 6. However, in Fig. 6 the distribution is illustrated for the case where $\omega t = 0$. For completeness of the consideration, here we also consider the distribution for the case where $\omega t = \pi/2$, the epures of which are given in Fig. 17 for $T_{22}h/P_0$ (Fig. 17(a)), $v_2\mu h/(P_0c_2)$ (Fig. 17(b)) and $v_1\mu h/(P_0c_2)$ (Fig. 17(c)) in the case where $\omega = 100$ Hz, $h_d/h = 2$ and $h = 0.01$ m for various values of V/h . It follows from these epures that as a result of the plate moving, the symmetry of the values of $T_{22}h/P_0$ and $v_2\mu h/(P_0c_2)$, and the asymmetry of the values of $v_1\mu h/(P_0c_2)$ with respect to the point $x_1/h = 0$, are significantly violated.

This completes the analysis of the numerical results related to the influence of the problem parameters, such as plate thickness, fluid depth, vibration phase and plate moving velocity on the frequency response of the stress and velocities.

The explanation of the numerical results or the describing of the real physical mechanism of the obtained numerical results can be based on the nature of the mechanical behavior of the

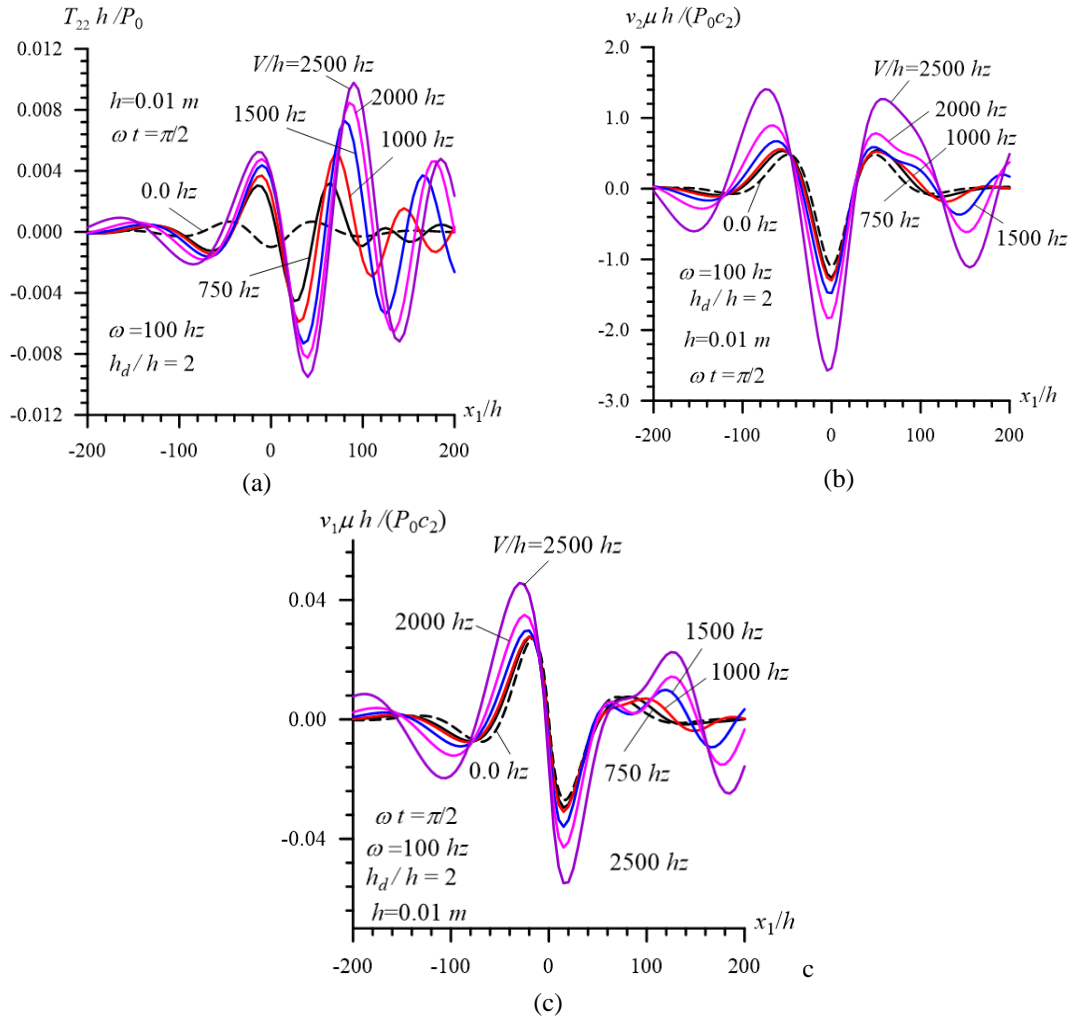


Fig. 17 Distribution of $T_{22}h/P_0$ (a), $v_2\mu h/(P_0c_2)$ (b) and $v_1\mu h/(P_0c_2)$ (c) with respect to x_1/h for various values of the plate moving velocity V/h in the case where $\omega t = \pi/2$, $\omega = 100$ Hz, $h = 0.01$ m and $h_d/h = 2$

simultaneously moving and vibrating deformable objects such as beams and plates (see, for instance, the papers by Lin and Qiao (2008), by Yang *et al.* (2010), Yao *et al.* (2016), Banichuk *et al.* (2010) and others listed therein). Note that the non-ordinary particularities, such as the appearing the critical frequencies (because such frequencies do not appear in the cases where axial moving velocity the plate is equal to zero), can be explained namely with the interaction between the axial moving velocity and the vibration. All the numerical results which are considered in the present paper are focused on the influence of the problem parameters on these particularities.

3.2 The influence of the fluid compressibility on the frequency response of the stress and velocities and on the values of the critical frequencies

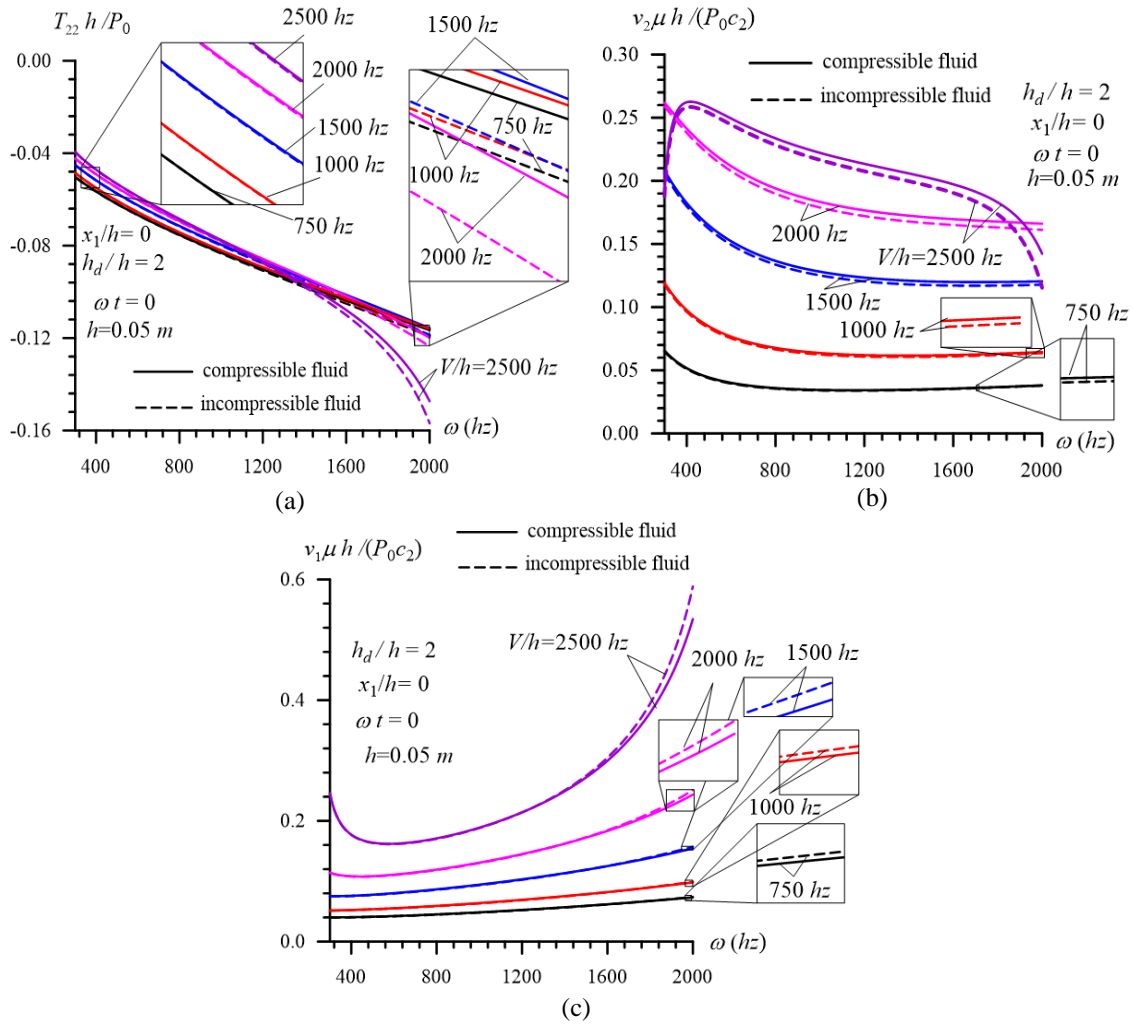


Fig. 18 The influence of the fluid compressibility on the frequency response of $T_{22}h/P_0$ (a), $v_2\mu h/(P_0c_2)$ (b) and $v_1\mu h/(P_0c_2)$ (c) for various values of the plate moving velocity V/h in the case where $h=0.05\text{ m}$, $h_d/h=2$, $\omega t=0$ and $x_1/h=0$

As has been noted above, the degree of fluid compressibility can be estimated through the parameter Ω_1 in Eq. (25). Consequently, the $\Omega_1=0$ case (i.e., the $a_0=\infty$ case) corresponds to the incompressible fluid model. Numerical results show that for the selected fluid, in the cases where $h\leq 0.03$, $4\text{ hz}\leq\omega\leq 1000\text{ hz}$ and $0\leq V/h\leq 1000\text{ hz}$, the influence of the fluid compressibility on the frequency response of the hydro-elastic system under consideration is insignificant and can be neglected with accuracy to the order ($\leq 10^{-6}$). Therefore, we carry out the investigation on the influence of the fluid compressibility on the studied frequency responses for the cases where $0.05\leq h\leq 0.1$, $300\text{ hz}\leq\omega\leq 2000\text{ hz}$ and $750\text{ hz}\leq V/h\leq 2500\text{ hz}$.

Thus, consider the graphs in Figs. 18 and 19 which are constructed for $\omega t=0$ and $\omega t=\pi/2$, respectively. Note that in these figures the graphs grouped by the letters a, b and c correspond to

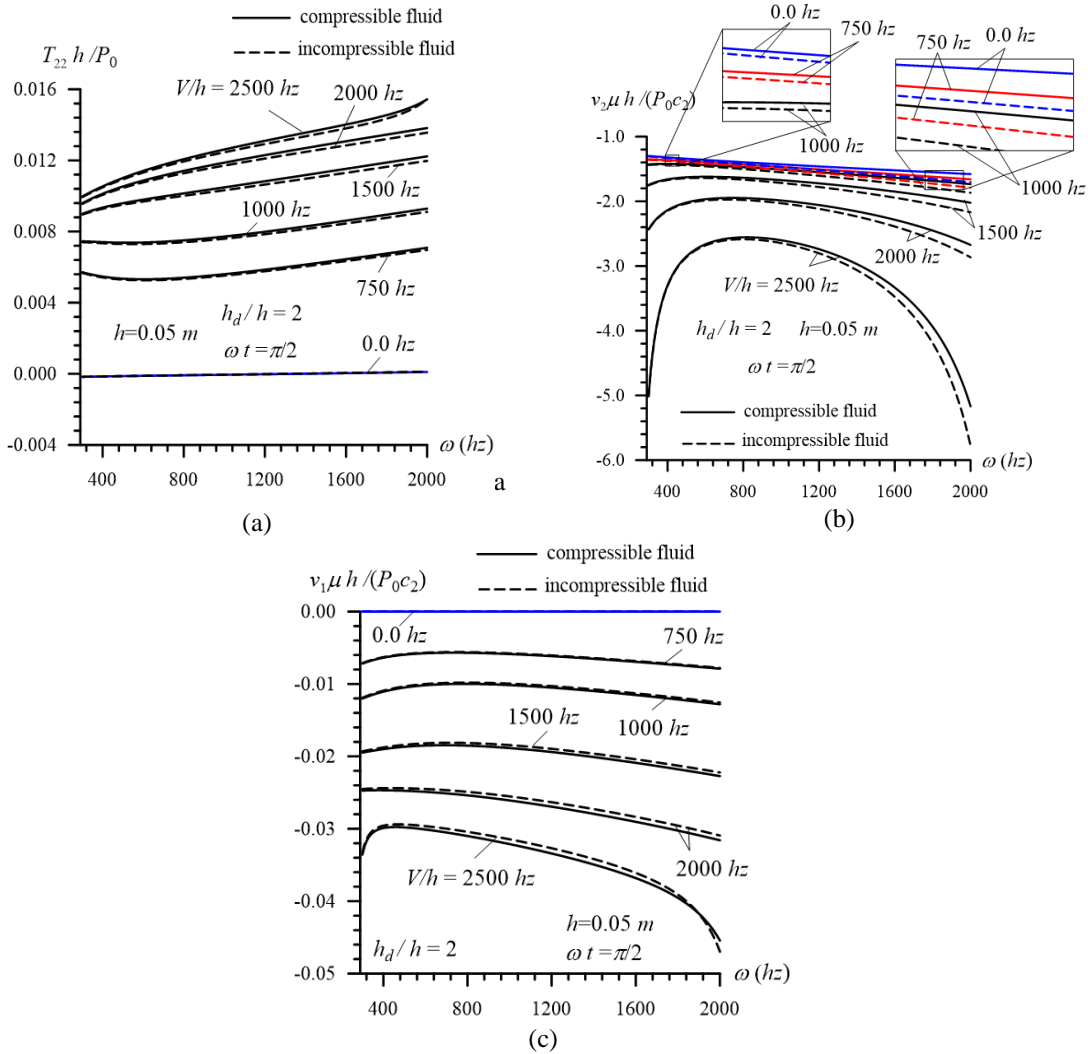


Fig. 19 The influence of the fluid compressibility on the frequency response of $T_{22}h/P_0$ (a), $v_2\mu h/(P_0c_2)$ (b) and $v_1\mu h/(P_0c_2)$ (c) for various values of the plate moving velocity V/h in the case where $h=0.05\text{ m}$, $h_d/h=2$, $\omega t = \pi/2$ and $x_1/h=0$

the quantities $T_{22}h/P_0$, $v_2\mu h/(P_0c_2)$ and $v_1\mu h/(P_0c_2)$, respectively. Moreover, note that in these figures the graphs related to the compressible and incompressible fluid models are given simultaneously and these graphs are constructed in the case where $h=0.05\text{ m}$, $h_d/h=2$ and $x_1/h=0$ for various values of the plate moving velocity V/h . It follows from the results that, as predicted above, the influence of the fluid compressibility on the studied frequency responses increases with the vibration frequency ω and with the plate moving velocity V/h . Moreover, the results show that the magnitude of the aforementioned influence increases with plate thickness h and becomes more considerable in the near vicinity of ω''_{cr} . These conclusions are also confirmed with the graphs given in Fig. 20 which are constructed within the scope of the assumptions and notation accepted

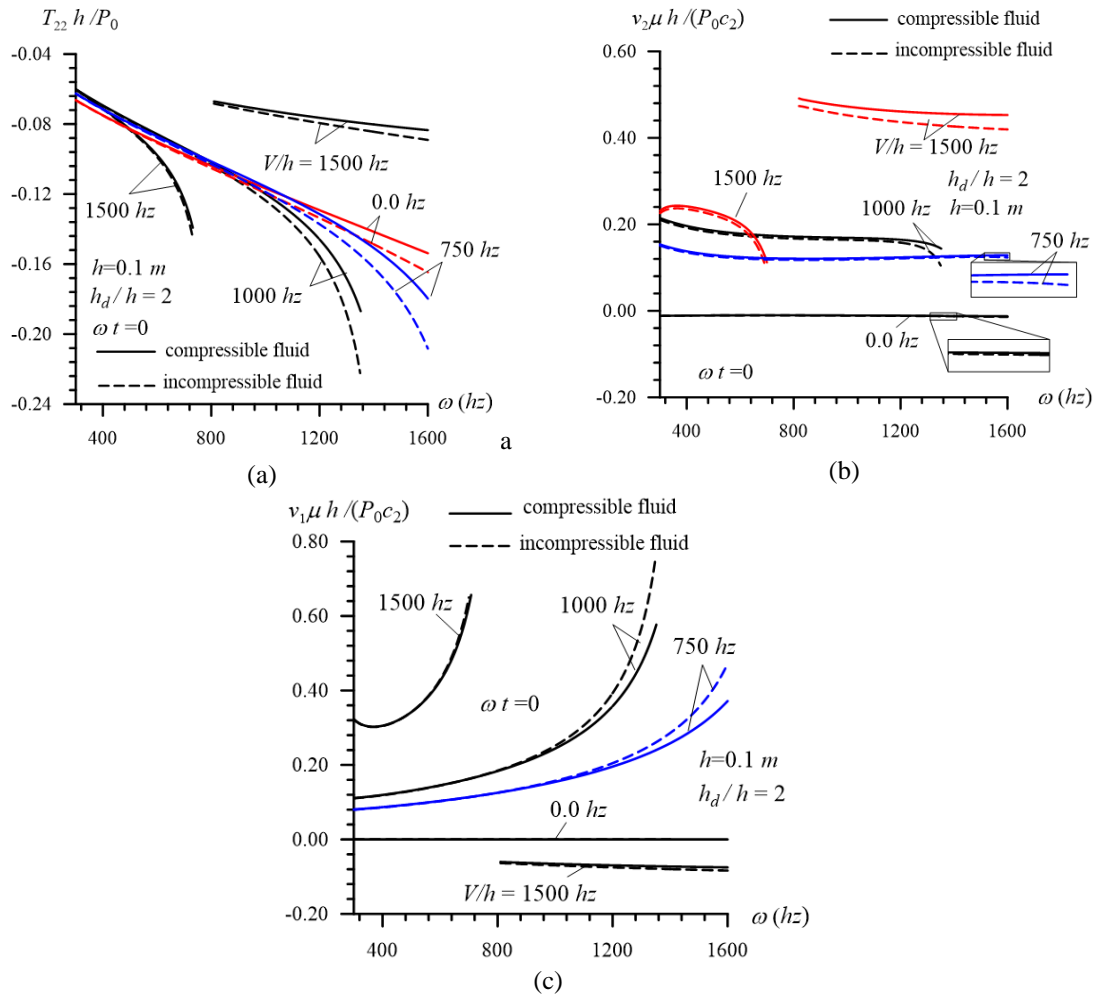


Fig. 20 The influence of the fluid compressibility on the frequency response of $T_{22}h/P_0$ (a), $v_2\mu h/(P_0c_2)$ (b) and $v_1\mu h/(P_0c_2)$ (c) for various values of the plate moving velocity V/h in the case where $h = 0.1\text{ m}$, $h_d/h = 2$, $\omega t = 0$ and $x_1/h = 0$

in Fig. 18 for the case where $h=0.1\text{ m}$. For clarity of the illustration in Fig. 20, the part of the graphs regarding the interval $(\omega''_{cr}-\delta, \omega''_{cr}+\delta)$ and constructed for the case where $V/h=1500\text{ hz}$ is removed.

According to the foregoing results, it can be concluded that in the cases where $400\text{ hz} < \omega < \omega''_{cr}$, in general, the fluid incompressibility causes an increase (a decrease) in the absolute values of $T_{22}h/P_0$ and $v_1\mu h/(P_0c_2)$ (of $v_2\mu h/(P_0c_2)$). Moreover, according to these results, it can be concluded that the fluid incompressibility causes a decrease in the values of ω''_{cr} . These conclusions are more clearly observed from the results given in Fig. 20.

Note that the results discussed in the present subsection are obtained in the case where $h_d/h=2$. Now we consider the numerical results which illustrate how an increase in the values of h_d/h affects the values of ω'_{cr} and ω''_{cr} within the scope of the compressible and incompressible fluid

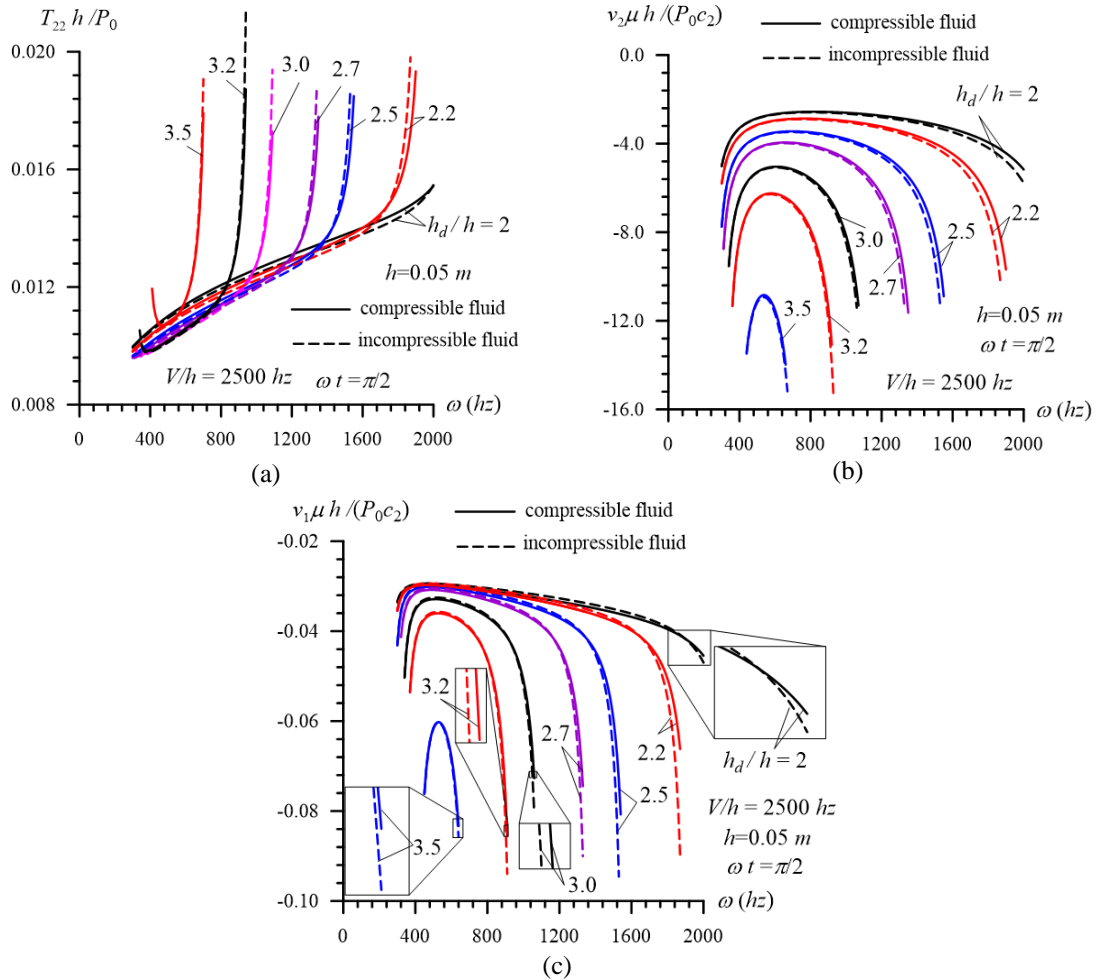


Fig. 21 The influence of the fluid depth parameter h_d/h under $2 \leq h_d/h \leq 3.5$ on the frequency response of $T_{22}h/P_0$ (a), $v_2\mu h/(P_0c_2)$ (b) and $v_1\mu h/(P_0c_2)$ (c), on ω'_{cr} and ω''_{cr} , and on the effect of the fluid compressibility on this influence in the case where $h = 0.05\text{ m}$, $V/h = 2500\text{ hz}$, $\omega t = \pi/2$ and $x_1/h = 0$

models. These results are given in Figs. 21 and 22 which are obtained for various values of h_d/h in the case where $\omega t = \pi/2$, $h = 0.05\text{ m}$, $V/h = 2500\text{ hz}$ and $x_1/h = 0$. Note that for clarity of the illustration, the results obtained in the cases where $2 \leq h_d/h \leq 3.5$ and where $3.5 \leq h_d/h \leq 5$ are given separately in Figs. 21 and 22, respectively. Moreover, note that in these figures, as in the foregoing ones, the graphs grouped by the letters a, b and c relate to $T_{22}h/P_0$, $v_1\mu h/(P_0c_2)$ and $v_2\mu h/(P_0c_2)$, respectively. In Fig. 21 in the cases where $h_d/h > 2$ the results are presented for the case where $\omega'_{cr} < \omega < \omega''_{cr}$, however, in Fig. 22 the results obtained for the cases where $h_d/h = 3.5$ and 3.7 are presented for $\omega \gg \omega''_{cr}$. At the same time, in Fig. 22 the results obtained for the cases $h_d/h = 4$ and 5 are presented for $80\text{ hz} < \omega < 1500\text{ hz}$.

Thus, it follows from the results given in Figs. 21 and 22 that an increase in the values of h_d/h causes a decrease in the values of ω''_{cr} and that with an increase in ω'_{cr} (although this increase is

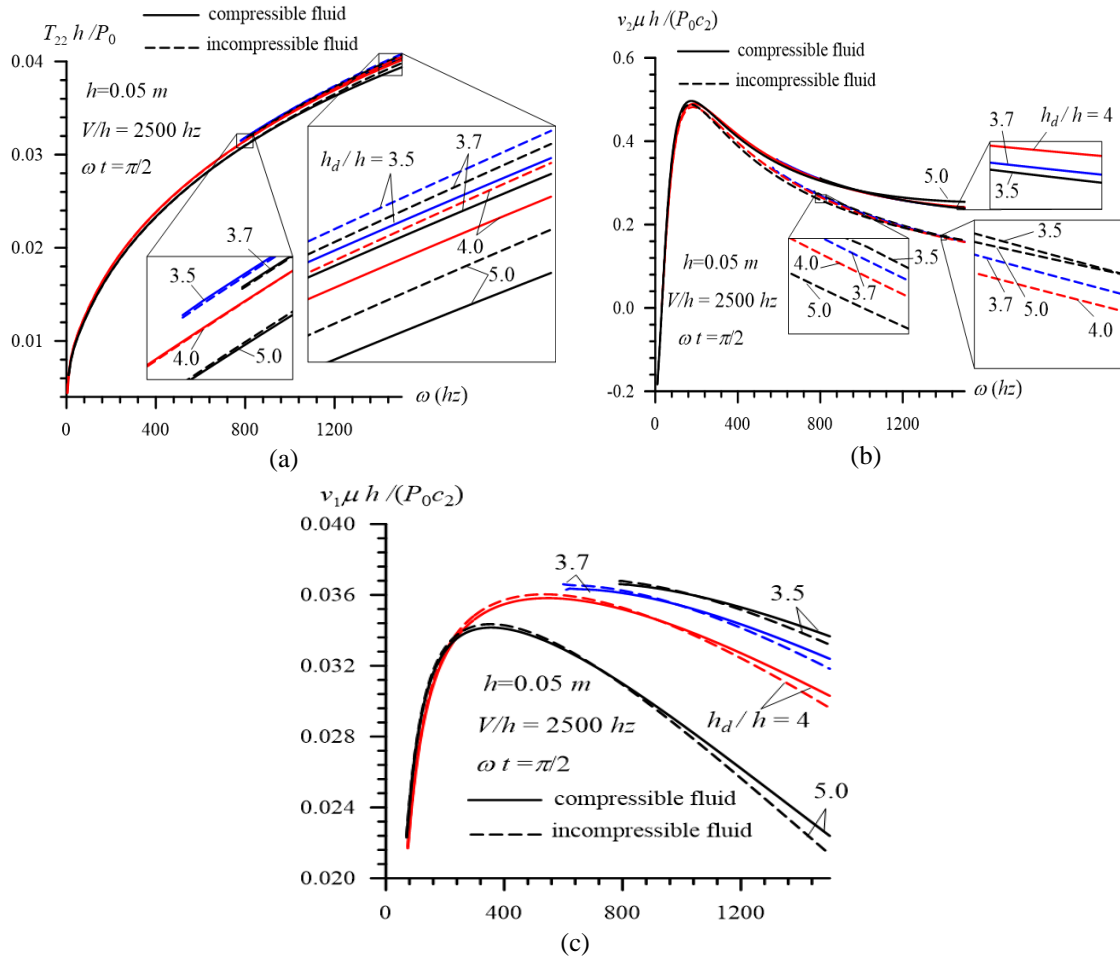


Fig. 22 The influence of the fluid depth parameter h_d/h under $3.5 \leq h_d/h \leq 5$ on the frequency response of $T_{22}h/P_0$ (a), $v_2\mu h/(P_0c_2)$ (b) and $v_1\mu h/(P_0c_2)$ (c), on ω'_{cr} and ω''_{cr} , and on the effect of the fluid compressibility on this influence in the case where $h=0.05\text{ m}$, $V/h=2500\text{ hz}$, $\omega t = \pi/2$ and $x_1/h=0$

insignificant), and after a certain h_d/d (denote it by $(h_d/d)^*$), i.e., under $h_d/h \geq (h_d/h)^*$, the critical frequencies disappear. For instance, in the case under consideration for $h_d/h \geq 4$ there is no critical frequency. Moreover, it follows from these results that the fluid incompressibility causes a decrease in the values of the second critical frequency ω''_{cr} .

We recall that in the case where $h=0.01$ we ascertained that the influence in the values of h_d/h on the values of the first critical frequency ω'_{cr} is insignificant and causes these values to decrease (see Fig. 12). However, the results given in Fig. 21 show that in the relatively thick plates, for instance, in the case where $h=0.05$ the influence of h_d/h on the values of the first critical frequency ω'_{cr} becomes more considerable and causes these values to increase. Nevertheless, the results show that the influence of h_d/h on the values of the second critical frequency ω''_{cr} is more considerable than on the first critical frequency ω'_{cr} .

This completes consideration of the numerical results and their analyses.

4. Conclusions

Thus, in the present paper some particularities of the forced vibration of the hydro-elastic system consisting of the axially moving elastic plate, compressible viscous fluid and rigid wall are studied by employing the discrete-analytical approach proposed in the previous work by the authors, Akbarov and Panakhli (2015). Numerical results on the frequency response of the stress and velocities on the interface plane between the fluid and plate are presented and discussed. These results illustrate the influence of the problem parameters such as the plate moving velocity, fluid depth, plate thickness, vibration frequency and the fluid compressibility on these responses. Concrete numerical results are obtained for the case where the plate material is steel and the fluid is glycerin. According to these results and their discussion, we can draw the following main conclusions.

- As a result of the fluid flow caused by the plate which is axially moving with constant velocity in the initial state within the scope of certain conditions, the first and second critical frequencies denoted by ω'_{cr} and ω''_{cr} , respectively, arise and under these critical frequencies a resonance-type phenomenon occurs;
- Under a fixed value of the fluid depth parameter h_d/h (see Fig. 1), the values of ω'_{cr} increase, but the values of ω''_{cr} decrease with the plate thickness h and after a certain value of this thickness, the critical frequencies disappear;
- For relatively thick plates, for instance, for the cases where $h \geq 0.05$ m, under a fixed value of the plate thickness h , the values of ω'_{cr} increase, but the values of ω''_{cr} decrease with the fluid depth parameter h_d/h and after a certain value of this parameter, the critical frequencies disappear;
- For each of the values of the plate thickness, the values of ω'_{cr} increase, but the values of ω''_{cr} decrease with the plate moving velocity and after a certain value of this velocity, the critical frequencies disappear;
- The influence of the fluid compressibility on the values of the first critical frequency is ω'_{cr} insignificant, but this influence is considerable for the second critical frequency ω''_{cr} and causes its values to increase;

Besides the foregoing general conclusions, according to the presented graphs, more concrete conclusions can be made related to the influence of the problem parameters on the values of the studied stress and velocities. For instance, it can be concluded that an increase in the values of the plate moving velocity causes the absolute values of the studied stress and velocities to increase; as a result of the fluid depth parameter h_d/h increasing the absolute values of the stress decrease, but absolute values of the velocities increase; the fluid compressibility causes the absolute maximum values of the studied stress to decrease.

It should be noted that the foregoing results on the critical frequencies arise as a result of the fluid moving in the initial (i.e., in the unperturbed) case and in the present paper the very simple flow case is considered. Consequently, investigations of related hydro-elastic problems with more complicated initial flowing cases also have a great impact in the theoretical and application senses. Therefore, the authors aim to continue related studies, namely for these complicated initial-flow cases.

References

- Akbarov, S.D. (2015), *Dynamics of Pre-strained Bi-Material Elastic Systems: Linearized Three-*

Dimensional Approach, Springer.

- Akbarov, S.D. and Ismailov, M.I. (2014), "Forced vibration of a system consisting of a pre-strained highly elastic plate under compressible viscous fluid loading", *CMES: Comput. Model. Eng. Sci.*, **97**(4), 359-390.
- Akbarov, S.D. and Ismailov, M.I. (2017), "The forced vibration of the system consisting of an elastic plate, compressible viscous fluid and rigid wall", *J. Vibr. Contr.*, **23**(11), 1809-1827.
- Akbarov, S.D. and Ismailov, M.I. (2015), "Dynamics of the moving load acting on the hydro-elastic system consisting of the elastic plate, compressible viscous fluid and rigid wall", *CMC: Comput. Mater. Contin.*, **45**(2), 75-105.
- Akbarov, S.D., Guliyev, H.H. and Yahnioglu, N. (2016), "Natural vibration of the three-layered solid sphere with middle layer made of FGM: Three-dimensional approach", *Struct. Eng. Mech.*, **57**(3), 239-263.
- Akbarov, S.D. and Panakhli, P.G. (2015), "On the discrete-analytical solution method of the problems related to the dynamics of hydro-elastic systems consisting of a pre-strained moving elastic plate, compressible viscous fluid and rigid wall", *CMES: Comput. Model. Eng. Sci.*, **108**(4), 89-112.
- Bagno, A.M. (2015), "The dispersion spectrum of wave process in a system consisting of an ideal fluid layer and a compressible elastic layer", *Appl. Mech.*, **51**(6), 52-60.
- Bagno, A.M., Guz, A.N. and Shchuruk, G.L. (1994), "Influence of fluid viscosity on waves in an initially deformed compressible elastic layer interacting with a fluid medium", *Appl. Mech.*, **30**(9), 643-649.
- Bagno, A.M. and Guz, A.N. (1997), "Elastic waves in prestressed bodies interacting with fluid (survey)", *Appl. Mech.*, **33**(6), 435-465.
- Banichuk, N., Jeronen, J., Neittaanmaki, P. and Tuovinen, T., (2010), "On the instability of an axially moving elastic plate", *J. Sol. Struct.*, **47**(1), 91-99.
- Charman, C.J. and Sorokin, S.V. (2005), "The forced vibration of an elastic plate under significant fluid loading", *J. Sound Vibr.*, **281**, 719-741.
- Fu, S., Cui, W., Chen, X. and Wang, C. (2005), "Hydroelastic analysis of a nonlinearity connected floating bridge subjected to moving loads", *Mar. Struct.*, **18**, 85-107.
- Fu, Y. and Price W. (1987), "Interactions between a partially or totally immersed vibrating cantilever plate and surrounding fluid", *J. Sound Vibr.*, **118**(3), 495-513.
- Guz, A.N. (2009), *Dynamics of Compressible Viscous Fluid*, Cambridge Scientific Publishers.
- Guz, A.N. and Makhort, F.G. (2000), "The physical fundamentals of the ultrasonic nondestructive stress analysis of solids", *Appl. Mech.*, **36**, 1119-1148.
- Guz, A.N. (2004), *Elastic Waves in Bodies with Initial (Residual) Stresses*, Kiev, A.C.K.
- Ilhan, N. and Koç, N. (2015), "Influence of polled direction on the stress distribution in piezoelectric materials", *Struct. Eng. Mech.*, **54**, 955-971.
- Kwak, H. and Kim, K. (1991), "Axisymmetric vibration of circular plates in contact with water", *J. Sound Vibr.*, **146**, 381-216.
- Lamb, H. (1921), "Axisymmetric vibration of circular plates in contact with water", *Proc. R Soc.*, **A98**, 205-216.
- Lin, W. and Qiao, N. (2008), "Vibration and stability of an axially moving beam immersed in fluid", *J. Sol. Struct.*, **45**(5), 1445-1457.
- Gao, L.G., Zhang, P., Liu, J. and Wang, W. (2016), "Elastic solutions due to a time-harmonic point load in isotropic multi-layered media", *Struct. Eng. Mech.*, **57**(3), 327-355.
- Sorokin, S.V. and Chubinskij, A.V. (2008), "On the role of fluid viscosity in wave propagation in elastic under heavy fluid loading", *J. Sound Vibr.*, **311**, 1020-1038.
- Tubaldi, E. and Armabili, M. (2013), "Vibrations and stability of a periodically supported rectangular plate immersed in axial flow", *J. Flu. Struct.*, **39**, 391-407.
- Wang, C., Fu, S. and Cui, W. (2009), "Hydroelasticity based fatigue assessment of the connector for a ribbon bridge subjected to a moving load", *Mar. Struct.*, **22**, 246-260.
- Wu, J.S. and Shih, P.Y. (1998), "Moving-load-induced vibrations of a moored floating bridge", *Comput. Struct.*, **66**(4), 435-461.

- Yang, X.D., Chen, L.Q. and Zu, J.W. (2010), "Vibration and stability of an axially moving rectangular composite plate", *J. Appl. Mech.*, **78**(1), 011018.
- Yao, G., Zhang, Y.M., Li, C.Y. and Yang, Z. (2016), "Stability analysis and vibration characteristics of an axially moving plate in aerothermal environment", *Acta Mech.*, **227**, 3517.
- Yao, G., Zhang, Y.M., Li, C.Y. and Yang, Z. (2016), "Stability analysis and vibration characteristics of an axially moving plate in aerothermal environment", *Acta Mech.*, **227**, 3517.
- Zhao, J. and Yu, S. (2012), "Effect of residual stress on the hydro-elastic vibration on circular diaphragm", *World J. Mech.*, **2**, 361-368.

CC

Appendix

In this appendix we give Table which contains the notation for parameters used in the paper and their physico-mechanical meaning.

Table of the used notation and their meaning

Notation	Meaning
x_1 and x_2	Coordinates of the points in the moving coordinate system Ox_1x_2
x_{10} and x_{20}	Coordinates of the points in the fixed coordinate system $O_0x_{10}x_{20}$
v_1 and v_2	Components of the fluid flow velocity vector in the moving coordinate system Ox_1x_2
t	The time
v_{10} and v_{20}	Components of the fluid flow velocity vector in the fixed coordinate system $O_0x_{10}x_{20}$
σ_{11} , σ_{12} and σ_{22}	Components of the stress tensor in the plate in the moving coordinate system Ox_1x_2
ε_{11} , ε_{12} and ε_{22}	Components of the strain tensor in the plate in the moving coordinate system Ox_1x_2
u_1 and u_2	Components of the displacement vector in the plate in the moving coordinate system Ox_1x_2
ρ	Mass density of the plate material
h	The plate thickness
h_d	The fluid depth
λ and μ	Lame constants of the plate material
$\rho_0^{(1)}$	Mass density of the fluid in the case where this fluid is rest
$\mu^{(1)}$	The coefficient of the fluid viscosity
$\lambda^{(1)}$	The second coefficient of the fluid viscosity
$p^{(1)}$	Perturbation of the pressure in the fluid
$\rho^{(1)}$	Perturbation of the mass density of the fluid
T_{11} , T_{12} and T_{22}	Components of the stress tensor in the fluid
e_{11} , e_{12} and e_{22}	Components of the strain velocity tensor
V	Axial moving velocity of the plate
ω	Angular frequency of the external time-harmonic force
s	Fourier transformation parameter
P_0	The amplitude the external time harmonic force
$\nu^{(1)} = \mu^{(1)} / \rho_0^{(1)}$	The coefficient of the kinematic viscosity of the fluid